Embryology and Classification of Congenital Upper Limb Anomalies

1

Carlos Garrido-Allepuz Herrera, Michael A. Tonkin, and Kerby C. Oberg

Morphological Overview

In vertebrates, the limb bud starts as an accumulation of cells within the lateral plate mesoderm (LPM) forming an oblong ventrolateral bulge on the body wall. The limb is a composite structure of cells from the LPM (precursors of limb-associated skeletal tissues) and associated somites (muscle and vascular precursors). In humans, the upper limb bud appears during the fourth week of development around day 26 (Carnegie stage 12) and is located between somites 9 and 12 (Fig. 1.1a) [1, 2]. The limb emerges only in certain zones of the body known as limb fields. The position of limb fields are thought to be specified by a quantitative and/or qualitative combination of Hox transcription factors (see Fig. 1.1b) [3, 4].

By day 37 of development (Carnegie stage 16), the distal portion of the limb can be recognized as a handplate. At the same time there is progressive mesodermal condensation along the proximodistal axis forming the skeletal elements of the limb. By day 56 the major morphologic features of the limb are complete.

Limb Initiation

After the upper limb fields have been specified, induction of the limb bud occurs. The cells of the LPM located within the limb fields maintain active proliferation, while non-limb field LPM begins to divide more slowly [5]. Initially *Fgf10* is expressed broadly along the LPM, but just before the limb emerges, the domain of *Fgf10* expression becomes restricted to the limb fields. In chicken, the expression of *Tbx5* and *Wnt2b* in the LPM cells of the limb field are responsible for the induction of *Fgf10* in the presumptive limb (Fig. 1.2) [6–8]. Recent studies suggest that *Tbx5* expression can be induced and regulated by Hox transcription factors, suggesting a role for Hox genes in both positioning limb fields and initiating limb outgrowth [9]. Fgf10 through its receptor FgfrIIa has been shown to induce *Wnt3* and *Wnt3a* in prospective mouse and chick limb ectoderm, respectively. Concurrently, Bone Morphogenetic Protein (Bmp) signaling in the ventral ectoderm induces β-catenin competency in cells of the presumptive apical ectodermal ridge (AER) at the dorsal–ventral boundary [10, 11]. In turn, Wnt3 or Wnt3a induces *Fgf8* in a Wnt/β-catenin-dependent manner in the precursor cells of the AER [6, 12]. Fgf8 secreted from the recently formed AER maintains the expression of *Fgf10* in the mesoderm, establishing a positive regulatory loop that maintains proximal–distal growth [6, 12].

Another signaling molecule that is fundamental to the induction of the limb bud appears to be retinoic acid (RA), the active metabolite of vitamin A. This molecule is produced in the somites of the embryo by the enzyme Raldh2 [13–15]. RA restricts the early expression of Fgf8 within the heart field, which, in turn, permits the expression of *Tbx5* in the limb field to initiate forelimb development [16, 17]. Furthermore, RA has been shown to regulate the expression of *Hox* genes both in vitro and in vivo, which may contribute to limb field induction and/or positioning (see Fig. 1.2) [18, 19].

C.G.-A. Herrera, Ph.D.
Department of Molecular and Cellular Anatomy,
Instituto de Biomedicina y Biotecnologia de Cantabria (IBBTEC),
CSIC-SODERCAN-Universidad de Cantabria C/Albert Einstein,
22. 39011 (PTCAN), Santander, Cantabria 39, Spain
e-mail: arcanumes@hotmail.com

M.A. Tonkin, M.B.B.S., M.D., F.R.A.C.S., F.R.C.S. (Ed Orth)
Department of Hand Surgery and Peripheral Nerve Surgery,
Royal North Shore Hospital, The Children's Hospital at Westmead,
University of Sydney, Sydney, NSW 2065, Australia
e-mail: mtonkin@med.usyd.edu.au

K.C. Oberg, M.D., Ph.D. (✉)
Department of Pathology and Human Anatomy, Loma Linda
University Medical Center, Molecular Embryopathy Laboratory,
24785 Stewart St., Loma Linda, CA 92354, USA
e-mail: koberg@llu.edu

D.R. Laub Jr. (ed.), *Congenital Anomalies of the Upper Extremity: Etiology and Management*,
DOI 10.1007/978-1-4899-7504-1_1,

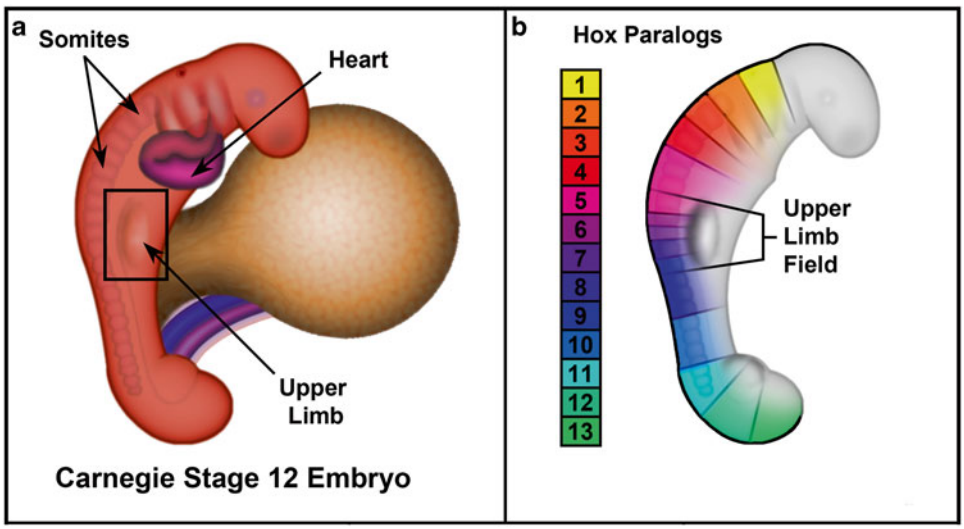

Fig. 1.1 Human embryo at stage of limb initiation and presumed Hox positioning. (**a**) Depiction of an emerging upper limb bud (boxed) in Carnegie stage 12 embryo. (**b**) Hox genes establish upper limb position and polarity. Courtesy of K.C. Oberg and Loma Linda University

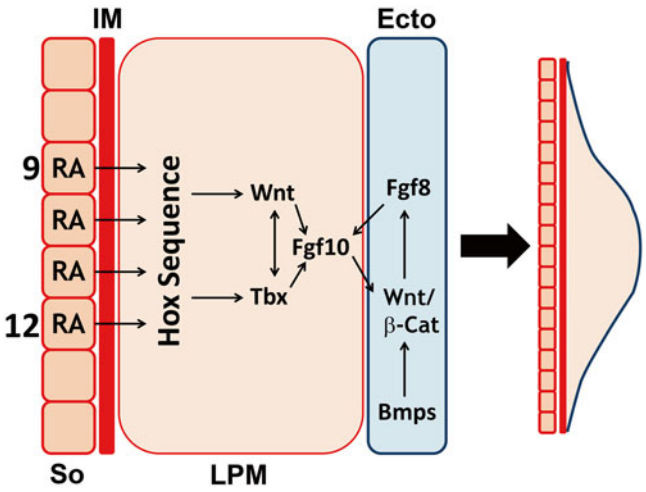

Fig. 1.2 Molecular pathways involved in limb induction. Depiction of the tissues involved in the initiation of the right upper limb bud emerging from lateral plate mesoderm (LPM) at somite (So) levels 9-12. Molecular interactions between LPM and ectoderm (Ecto) are also illustrated. IM-intermediate mesoderm. Courtesy of K.C. Oberg and Loma Linda University

Signaling Centers

Between the fourth and eighth weeks of development, the limb bud undergoes growth and differentiation to transform it into a fully patterned limb. This process can be described in terms of three coordinate axes: proximal–distal (P–D), anterior–posterior or radial–ulnar (A–P/R–U), and dorsal–ventral (D–V) modulated by three signaling centers [20].

Along the P–D axis, the AER appears as thickened ectoderm overlying the distal edge of the limb bud [21]. The AER is the signaling center that regulates the P–D growth and Fgfs are the signaling molecules that accomplish its function. Excision of the AER in chicken embryos at different stages of limb development results in limb truncations in a progressive fashion; the later the AER removal, the more distal the resulting truncation [22].

The signaling center for the A–P/R–U axis is the zone of polarizing activity (ZPA), a cluster of mesodermal cells located at the distal posterior (ulnar) margin. The ZPA directs A–P/R–U patterning and Shh is the signaling molecule that mediates its function. Both mice (*Shh* knock-out) that lack Shh function or mutant chickens (Oligozeugodactyly—*Ozd* mutants) that fail to have limb-specific Shh expression show marked loss of posterior (ulnar) elements [23, 24].

Dorsal non-AER ectoderm directs D–V patterning with Wnt7a as the signaling molecule that promotes dorsalization. Excision and rotation of the dorsal ectoderm results in the formation of dorsal structures within the ventral aspect of the limb [25].

Patterned Development Along Coordinate Axes

Pattern formation is a process by which the cells are sequentially specified, determined, and then differentiated to form the morphological structures of the limb. In this section we will focus on how the process of patterning is accomplished along each axis as directed by the signaling centers and the associated molecular pathways, recognizing that the molecular cascades of these three axes are operating concurrently and integrated together like a fine-tuned instrument.

Proximal–Distal Patterning (P–D)

The upper limb can be divided into three different segments along the P–D axis (Fig. 1.3): (1) the proximal segment or

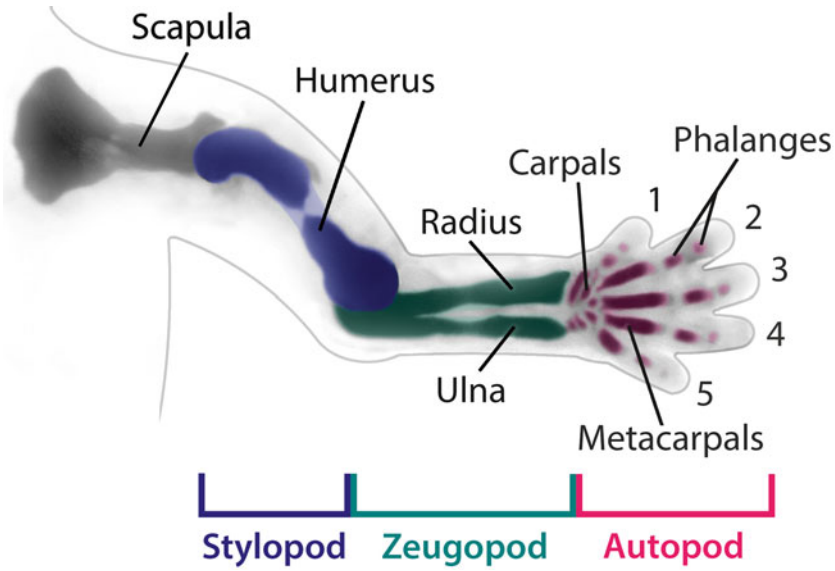

Fig. 1.3 Limb elements. The upper limb consists of a limb girdle or shoulder, and three limb segments known as the stylopod (humerus - colored blue), the zeugopod, which includes the radius and ulna (colored green) and the autopod or handplate (colored magenta). Courtesy of K.C. Oberg and Loma Linda University

stylopod where the skeletal elements of the humerus develop; (2) the intermediate segment or zeugopod where the radius and ulna form; and (3) the distal segment or autopod where the carpals, metacarpals, and digits form.

Patterning along the P–D axis begins during limb initiation with the formation of the AER, stratified ectoderm at the distal dorsal–ventral boundary of the developing limb bud. The AER secretes fibroblasts growth factors (Fgfs), the molecules primarily responsible for P–D patterning. Fgf8 is the first and functionally most important Fgf secreted from the AER during induction and maintained until the AER regresses, when the drafts of the last phalanges are formed. *Fgf4*, *Fgf9*, and *Fgf17* are activated sequentially in the posterior AER and expand to the anterior aspect as the limb develops [26, 27]. Classical experiments in chick embryos showed that AER removal abated distal limb outgrowth and resulted in truncations that corresponded to the timing of AER removal; in other words, the later the AER removal, the more distal the structures that were present [22]. Moreover, FGF-soaked beads were able to restore limb bud outgrowth and patterning after AER removal, indicating that Fgfs were the functional signaling factors of the AER [28, 29].

Among the different *Fgfs* expressed, *Fgf8* is thought to be the main AER signal, while *Fgf4*, *Fgf9*, or *Fgf17* are considered secondary or redundant [30, 31]. This concept is supported from experiments with *Fgf8* knock-out mice that showed smaller AERs, delayed limb bud outgrowth, and loss of some skeletal elements [26, 32]. In contrast, knock-out mice for *Fgf4*, *Fgf9*, and/or *Fgf17* did not develop limb anomalies. Interestingly, *Fgf4* expression in *Fgf8* knock-out mice was up-regulated, suggesting that redundant expression may have lessened the phenotype of these mutants. This was confirmed by the removal of both *Fgf4* and *Fgf8* that resulted in a worse phenotype with notably smaller limb buds [32, 33].

Several models have been proposed for P–D patterning. The progress zone model proposes that mesenchymal cell fate is determined by the length of time spent under the direct influence of the AER in a proliferative region called the progress zone (PZ) [34, 35]. The early specification model [36] postulates that the P–D identities are specified early and the different progenitor pools expand sequentially as the limb grows. The differentiation front model suggests that the AER maintains mesenchymal cells in an undifferentiated state; as the limb expands, the cells that are no longer under the influence of the AER differentiate [37].

However, the accumulating evidence supports an alternative model. The two signal model [30] proposes that two opposing signals pattern the limb along the P–D axis: RA emanating from the flank will specify a proximal fate, while Fgfs from the AER will specify a distal fate (Fig. 1.4a) [38, 39]. In somites, Raldh2 oxidizes Retinol to form RA which can act locally in the proximal limb buds to promote the expression of *Meis1* and *Meis2*. The expression of *Meis1*/2 defines the proximal limb segment and where the humerus (stylopod) will develop. Distally, Fgf signaling induces 5′*Hoxa* genes (*Hoxa11*, *Hoxa13*) and limits distal *Meis1*/*2* expression. Although the mechanism for this repression is not fully understood, it is known that Fgf8 signaling induces the expression of *Cyp26b1* in the distal mesenchyme of the limb bud; the product of this gene oxidizes RA into a non-active form, thus clearing the distal region of active RA (see Fig. 1.4c) [40]. Some have questioned RA role as a proximalizing agent [16], and further investigations are warranted to clarify whether RA or another factor influenced by RA is the proximalizing signal.

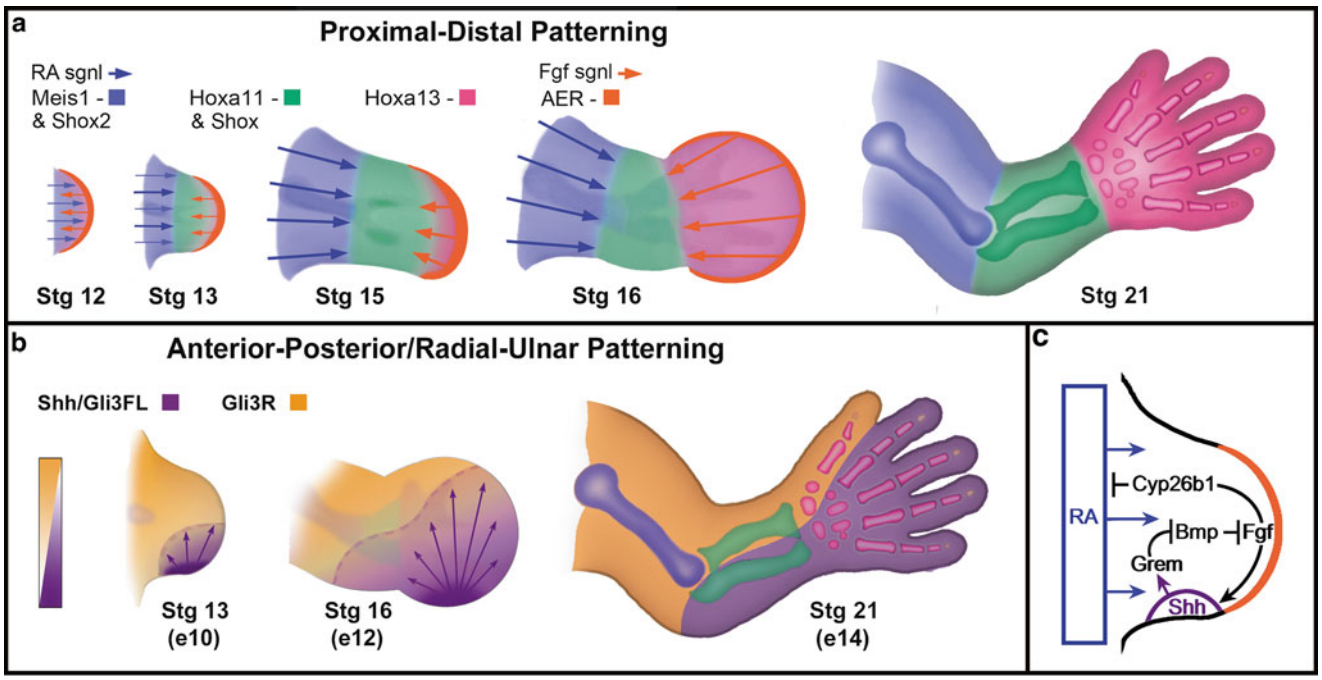

Fig. 1.4 Molecular pathways regulating proximal-distal & anterior-posterior/radial-ulnar axes. (**a**) Progressive segment specification along the proximal-distal axis based on the two signal model with RA-related proximalizing signals countered by distalizing Fgf signals. Outgrowth separates the signals and an intermediate zone is formed. Mies1 and Shox2 are restricted to the stylopod, Hoxa11 and Shox are markers for the zeugopod, and Hoxa13 delimits the handplate boundaries. (**b**) Opposing gradients of Gli3 repressor (Gli3R) and Shh-maintained full length Gli3 activator (Gli3FL) establish boundaries between the radius and ulna in the zeugopod and the thumb and ulnar digits in the autopod or hand. c) Some of the molecular interactions that maintain and terminate Shh expression in the ZPA (→ indicates positive regulation, while –| indicates inhibition). Courtesy of K.C. Oberg and Loma Linda University

Anterior–Posterior/Radial–Ulnar Patterning (A–P/R–U)

The limb along the A–P/R–U axis is divided into two segments: the anterior (radial), comprises the thumb and radius, and the posterior (ulnar) with the ulna and ulnar digits (digits two through five) [41].

Patterned development along the A–P/R–U axis is controlled by the zone of polarizing activity (ZPA), a cluster of mesenchymal cells maintained in the distal posterior/ulnar aspect of the developing limb (see Fig. 1.4b). The ZPA was discovered in 1968 through grafting experiments in chick limb buds [42]. In these experiments, grafts from the distal posterior/ulnar mesenchyme were excised from one group of chicks and then inserted into the distal anterior/radial aspect of another group of chicks. The limbs that developed from these grafts demonstrated mirror image duplication of structures [42–44]. RA was found to be the first molecule that mimicked ZPA grafts when applied to the distal anterior/radial aspect of the limb bud [45–48]. Later it was shown that Shh was the molecule responsible for the phenotype induced by RA [49].

Shh is critical to the correct developmental pattern of the limb, particularly for the forearm (zeugopod) and hand (autopod). This is demonstrated in *Shh* knock-out mice, which have a correctly developed stylopod, a single skeletal element (radius) for the zeugopod, and a minimal autopod. In the upper limb, the autopod forms as a small cartilage condensation [23, 50], while in the lower limb, the autopod consists of a single digit with two phalanges [23, 50].

A–P/R–U polarity and subsequent Shh expression is initiated by axial Hox gene segmentation [51] followed by several other factors that contribute to Shh induction and the establishment of the ZPA. Hand2, expressed in the posterior/ulnar half of the limb bud, is required for Shh induction [52, 53] and has been shown to directly interact with limb-specific Shh regulatory region [54]. Similarly, distal Hoxd (Hoxd10-13) transcription factors also interact with the limb-specific Shh regulatory region, and evidence suggests that their initial phase of limb bud expression helps to localize Shh expression (Fig. 1.5) [55].

The first or initial phase of distal Hoxd expression in the limb bud occurs in a nested collinear (corresponding to their gene order) fashion along the anterior–posterior axis, with Hoxd10 exhibiting the broadest initial expression domain. The expression of each successively more distal Hoxd gene is nested within the previous gene's expression domain (see Fig. 1.5). Hoxd13, the terminal transcription factor in the Hoxd cluster, has the most restricted expression domain within the distal posterior or ulnar aspect of the limb bud overlapping the ZPA. This first phase of distal Hoxd expression plays a role in localizing Shh expression and temporally corresponds to specification of the forearm or zeugopod.

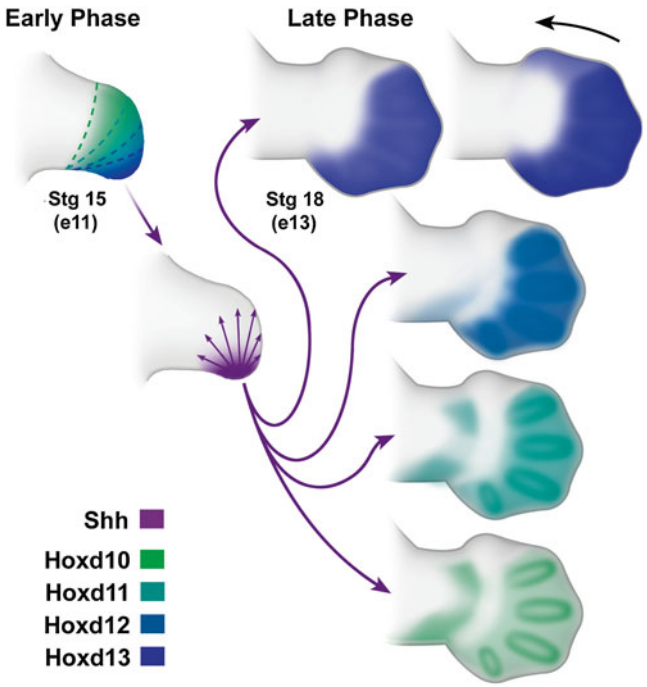

Fig. 1.5 Distal Hoxd genes are expressed in the limb bud in two phases. In the early phase, there is a nested collinear expression pattern. Dotted lines highlight the boundaries of expression, from broadest expression of Hoxd10 (green) to the most restricted of Hoxd13 (blue). In the late phase, Hoxd expressioin demonstrates quantitative colinearity with progressively more robust expression. Courtesy of K.C. Oberg and Loma Linda University

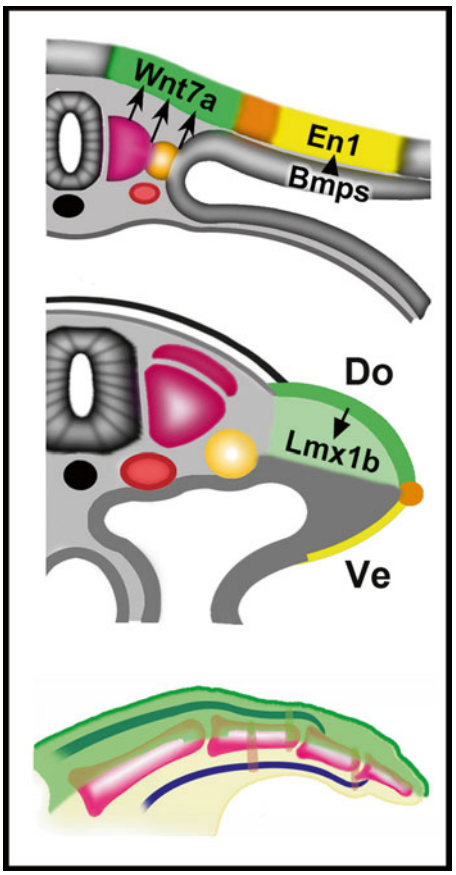

Fig. 1.6 Molecular pathways regulating the dorsal-ventral axis. From top to bottom, unknown factors in somites and/or intermediate mesoderm initiate Wnt7a expression in medial dorsal ectoderm. Bmps induce the expression of En1 in what will become the ventral ectoderm establishing the dorsal ventral boundary where the AER will form (orange). Wnt7a will induce Lmx1b in the underlying mesoderm to dorsalize developing tendons, joints and soft tissues. Courtesy of K.C. Oberg and Loma Linda University

The role of Shh in A–P/R–U axis patterning has been characterized largely through knock-out mice for members of the Gli protein family of transcription factors (Gli1, Gli2, and Gli3). *Gli3* mutant mice are polydactylous without digit identity while the zeugopod is perfectly formed [56, 57]. Remarkably, the limbs of the double knock-out mice for both *Gli3* and *Shh* were indistinguishable from the *Gli3* mutant alone [58, 59], suggesting that the principal function of Shh is mediated through Gli3. Molecular studies demonstrated that Shh signaling prevents the posttranslational processing of full-length Gli3 protein into a short form, which functions as a strong repressor of Shh target genes.

Secreted Shh diffusing from the ZPA establishes a posterior to anterior concentration gradient. A complementary gradient of Gli3R forms with high levels of Gli3R in the anterior zone where Shh signaling is minimal (see Fig. 1.4b) [59]. In the absence of *Shh*, the level of Gli3R is uniform along the A–P/R–U axis and the elevated levels of Gli3R, unopposed by Shh, are accompanied by an increase in the apoptotic rate of the limb mesenchyme [58, 60]. Thus, the A–P/R–U gradient of Gli3R and its reciprocal full length Gli3 activator are responsible for conveying pattern information along this axis. However, it remains unclear whether the critical patterning signal is the absolute level of GLi3R or the relative levels between the repressor and the activator forms [58, 59]. Collectively, these data help to characterize the role of Shh in A–P/R–U patterning which, at least, in part, is to regulate the form and function of its transcription factor, Gli3.

Dorsal–Ventral Patterning (D–V)

Patterning along this axis is regulated by signals from the non-AER ectoderm that surrounds the limb mesenchyme. The dorsal and ventral areas are defined by the expression of two different genes: *Wnt7a* in the dorsal ectoderm and *En-1* in the ventral ectoderm (Fig. 1.6). *Wnt7a* signaling defines the dorsal fate of the limb structures [61], while *En-1* restricts *Wnt7a* expression to the dorsal ectoderm, preventing the dorsalization of ventral limb tissues [62, 63]. It is not yet known how *Wnt7a* is induced in the presumptive limb ectoderm; however, there is evidence that BMP and WNT canonical signaling are responsible for the induction of *En-1* in the ventral ectoderm. Knock-out mice have further elaborated their functional roles. *Wnt7a* mutants have biventral limbs, while

En-1 mutants have bi-dorsal limbs [64, 65]. Interestingly, double compound mutant mice for *En-1* and *Wnt7a* display a biventral phenotype, suggesting that the default limb phenotype is ventral and establishing Wnt7a's role as the dorsalizing signaling molecule of the limb's D–V axis [64].

Additional studies demonstrate that *Wnt7a* manifests its function through the induction of *Lmx1b* in the underlying dorsal mesoderm. Lmx1b function is both sufficient and necessary for the induction of dorsal fates. In chicken and mice, ventral *Lmx1b* expression led to bi-dorsal limbs, whereas its inactivation resulted in biventral limbs [61, 64, 66, 67].

Integration of Axis-Related Signaling

The three signaling centers coordinate patterned limb development through interactions between their molecular signaling cascades. One of the most studied interactions is the interaction between the ZPA and the AER. Shh signaling from the ZPA induces the expression of *Gremlin* in the adjacent mesenchyme that underlies the AER [26]. Gremlin is an antagonist of BMP signaling, repressing *Bmp* expression in the mesenchyme [68, 69]. Although Bmp signaling is needed in limb and AER induction [70, 71], mesenchymal BMP inhibits the expression of AER-associated Fgfs and increases mesenchymal cell death [70, 71]. Thus, Shh through Gremlin prevents these BMP-associated functions thereby maintaining Fgf expression. Correspondingly, Fgf8 secretion into the mesenchyme maintains Shh expression in the ZPA (through pathways that are not yet characterized) forming a positive feedback loop that supports continued limb growth and patterning. Termination of this reciprocal loop has been proposed as the mechanism that stops limb outgrowth once the appropriate size has been achieved [72].

Integration also occurs between other axes. *Wnt7a* knockout mice shows a reduction in *Shh* expression [61] with a loss of the posterior digits (corresponding to the little finger). In chickens, elimination of the dorsal ectoderm of the limb showed similar results [73, 74]. These findings suggest that Wnt7a signaling from the dorsal ectoderm is capable of inducing or maintaining Shh expression in the ZPA [61]. Although the characterization of pathways that interconnect these three signaling centers is incomplete, it is intuitive that interaction between them is crucial for the proper development of a patterned limb.

Handplate Patterning

The handplate or autopod is the distal-most element of the limb and the last to form. It is composed of digits (fingers) and wrist bones. The axes-related pathways converge to form the most complicated, pattern-rich structures of limb development. Hoxa13, the terminal transcription factor of the Hoxa cluster, is confined to the handplate, demarcating its proximal boundary along the P–D axis (see Fig. 1.4a) [75, 76]. Concurrently, along the A–P/R–U axis, a second "late" Shh-regulated phase of distal Hoxd expression (that corresponds with digit formation) is generated that partially reverses their expression domains, i.e., reverse colinearity (see Fig. 1.5) [77]. More importantly, there is progressive expression intensity, with Hoxd13 exhibiting the most robust expression within the digits and Hoxd10 exhibiting the least intense expression, in what has been termed quantitative colinearity [78]. Along the D–V axis, expression of Lmx1b, the dorsalizing Wnt7a-mediated transcription factor, becomes restricted to dorsal tendons and joint-associated tissues (see Fig. 1.6) [79].

Establishing Digit Number

In addition to regulating the second phase of Hoxd gene expression in the limb bud, Shh-expressing ZPA cells also make a direct contribution to digit development. Fate mapping studies have demonstrated that descendants from Shh-expressing cells of the ZPA populate digit 5, 4 and half of digit 3. The cells of digit 5 have had the longest exposure to Shh and at higher levels, while the cells of the digit 2 are only affected by diffusion of Shh [80, 81]. Moreover, premature arrest in *Shh* expression causes a reduction in the number of digits corresponding to the stage and duration of arrest. With normal Shh levels, the order of condensation is d4, d2, d5, and d3, and with the premature arrest in shh, the loss follows a predictable order, where digit 3 is lost first, followed by d5, d2, and d4 [82]. Studies of digit duplication in chicken wings by *Shh* misexpression show that the most posterior/ulnar digits need higher Shh concentrations and longer exposure times than the more anterior digits [83].

Recent experiments in chicken show that Shh integrates both proliferation and specification of digit precursors and that Shh expression is controlled by cell proliferation [82, 84]. These data prompted two models to explain how digit morphology and number are achieved. The biphasic model suggests that an early phase specifies digit number and potential morphology and a second proliferative phase allows for digit growth and final morphologic determination [82]. The growth-morphogen model posits that both Shh concentration and exposure duration progressively expands the limb to specify digit number and morphology [84].

Although a Shh concentration gradient can account for some features of digit morphogenesis, it does not fully explain the repeating digit/interdigit pattern. Experiments out of Marian Ros' laboratory found that compound gene deletions of *Hoxa13* (the terminal *Hoxa* gene demarcating the handplate), *Hoxd11-13* (the Shh-dependent *Hox* genes of the A–P/R–U axis), and *Gli3* (the gene mediating Shh activity along the A–P/R–U axis) exposed an intrinsic self-organizing mechanism in mice involved in digit patterning

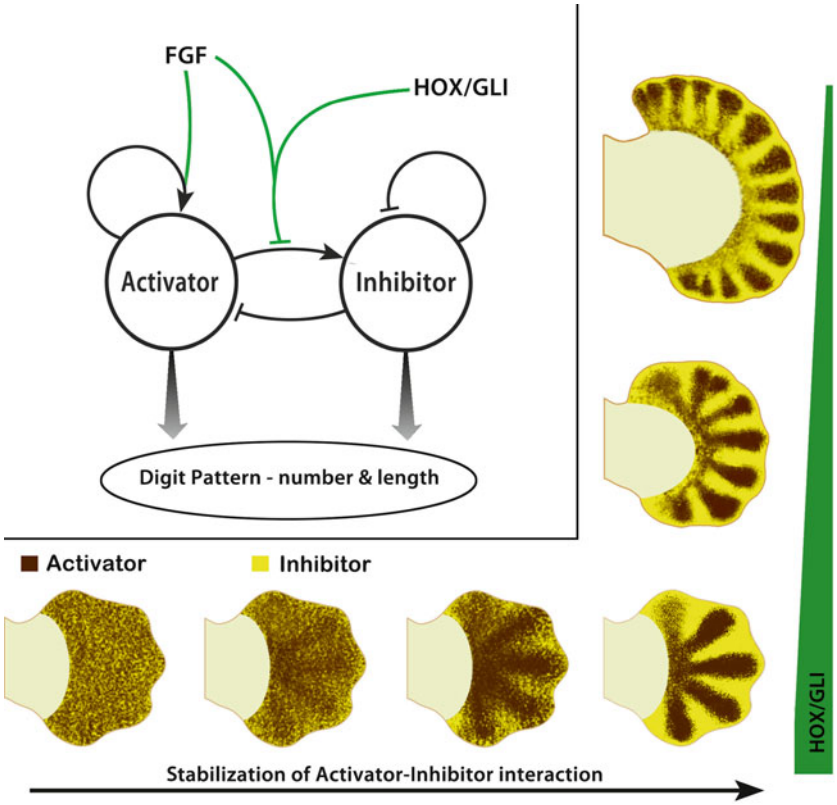

Fig. 1.7 Turing-like patterning in limbs. In the upper left-hand corner is a diagram of the diffusion-driven instability model with an activator and inhibitor modulated by FGF and HOX/GLI. In the model described by Sheth et al. (2012), FGF from the apical ectodermal ridge (AER) promotes a radial stripe pattern from this intrinsic self-organizing mechanism (ISOM) and ultimately regulates digit length, while FGF in concert with distal HOX and GLI transcription factors limit the number of digits. The bottom of the illustration has a series of handplates that show the rapid progression from fluctuating activator-inhibitor interaction (noise) to a stabilized 5-digit pattern. On the right, progressive loss of digit suppressing HOX/GLI transcription factors (green bar) causes an increase in the number of digits patterned by the ISOM. Courtesy of K.C. Oberg and Loma Linda University

[85]. Progressive reduction of the *Hox* gene dosage in the absence of Gli3 progressively increased digit numbers (up to 14 digits) that was not accompanied by a corresponding increase in handplate size; thus, the digits were increasingly thinner and shorter.

Alan Turing developed a mathematical diffusion-reaction model to account for repetitive self-organizing patterns, such as stripes or spots in animal skin and fur [86]. This model considers two molecules, an activator and inhibitor, which diffuse into a field of cells. The activator auto-up-regulates itself and up-regulates its own inhibitor. In contrast, the model's inhibitor suppresses the activator and auto-inhibits its own expression (Fig. 1.7).

Small random molecular variations of activator and inhibitor eventually lead to a stable pattern, typically spots or stripes. The pattern is dependent upon the level of activator and inhibitor as well as their diffusion rates. The evidence suggests that an intrinsic self-organizing or Turing mechanism establishes the initial alternating digit/non-digit pattern in the handplate. Although the identity of the activator and inhibitor are not yet known, the compound *Hox/Gli3* experiments indicate that the terminal Hoxa/d transcription factors involved in the P–D and A–P/R–U axes, in concert with Shh/Gli3 regulation, modulate the intrinsic self-organizing mechanism and are critical in establishing the common digit/interdigit pattern of pentadactyly.

Defining Digit-Specific Morphology

Once the number of digits has been established, each digit must then acquire its specific morphology, i.e., thumb and index finger. At the distal end of each digit is a cluster of cells called the phalanx forming region (PFR) or digital crescent that, with progressive digital outgrowth, regulates *Sox9* expression and chondrogenesis, thereby shaping phalangeal morphology (Fig. 1.8) [87–89]. The PFR also maintains digit-associated Fgf expression in the overlying AER during digit outgrowth [87].

Although the mechanisms are not fully characterized, evidence suggests that Shh plays a pivotal role in defining digit-specific morphology for digits 2–5 (the Shh-dependent digits). Three Shh-regulated gradients converge to define the appropriate size and number of phalanges. The Shh-dependent

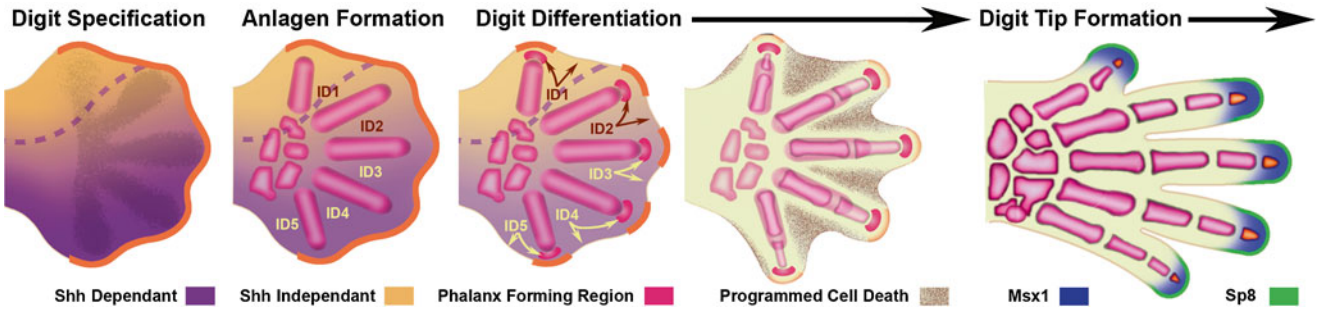

Fig. 1.8 Molecular pathways regulating digit development. After establishing digit number and the Shh dependant/independent domains (boundaries indicated by dashed line), digit morphologies are specified. Interdigital mesoderm as illustrated (ID1–ID5) regulates regression of the overlying AER (orange) and digit morphologies of the adjacent anterior condensing digit via the phalanx forming region (PFR—magenta) capping the distal tip of each anlagen. The PFR, in concert with the AER, determines phalanx size, length and joint position. The interdigital tissue subsequently undergoes Bmp mediated programmed cell death (speckled regions). As the AER overlying the digit regresses the distal or ungual phalanx begins to form and is demarcated by expression of mesodermal Msx1 (blue) and ectodermal Sp8 (green) (Image adapted from Oberg et al., 2010) [209]. Courtesy of K.C. Oberg and Loma Linda University

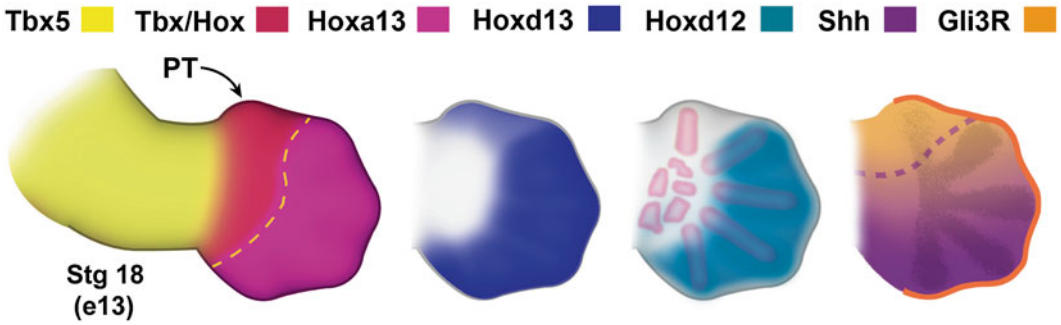

Fig. 1.9 Molecular regulation of thumb patterning. The presumptive thumb domain (PT) is defined by the overlapping expression of Tbx5, Gli3R, Hoxa13, and Hoxd13. The other Hoxd transcription factors (10-12) have overlapping expression domains in presumptive digits 2-5, but are restricted from the thumb domain. Note that the Hoxd genes are also restricted from the developing carpal region (Image modified from Oberg, 2014) [97]. Courtesy of K.C. Oberg and Loma Linda University

Hoxd10-13 transcription factors within the developing digits interact directly with Gli3 [90]. However, the form of Gli3 present at each digit varies based on the Shh-regulated Gli3R/Gli3 activator counter gradients [91]. In addition, Shh induces a Bmp gradient that is also known to regulate digit morphology [89, 92]. The signals that determine digit morphology are conveyed to the PFR through the adjacent posterior interdigital tissue [87, 89] and through Fgf and Wnt proteins secreted from the overlying AER [88, 93–96]. Changes in the interdigital BMP levels or swapping interdigital mesenchyme can transform digit morphology [87, 89].

The thumb is a distinctly different digit in its shape, position, and structure [97]. It is Shh-independent and has a compilation of genes expressed within its domain that is dissimilar from other digits (Fig. 1.9). *Hoxa13* is expressed within the entire handplate [75, 76] and overlaps the expression of *Tbx5*, which extends into the carpal and thumb domains but not into the domains of the ulnar digits (digits 2–5) [98]. Moreover, the thumb domain is accentuated by the lack of Shh-regulated *Hoxd10-12* expression [99]. The absence of distal *Hoxd* gene expression has been used as a marker of "thumbness" across species [100, 101]. Interestingly, the wrist is also a zone with limited Hox protein expression (see the illustration in Fig. 1.9 associated with Hoxd12 expression). Recent experiments with mouse mutants that express low levels of Hox proteins showed transformations of metacarpal bones to carpal-like elements [102]. Thus, Tbx5 and low levels of Hox transcription factors may limit the size of the thumb and carpal bones, while the distal Hoxd transcription factors are thought to elongate digits [75, 98, 103].

The terminal phalanges differ structurally from other phalanges: they are cone shaped and associated with a surface modification at the dorsal tip called the unguis or nail, which is dense keratinized epithelium that protects the tip of the digit. Terminal phalanges also differ in their development,

with ossification beginning at the distal tapered tip of the cartilage model rather than forming a collar around the midshaft [104]. As the AER regresses, the terminal phalanges begin to form [94, 105]. Sp8, a specificity protein transcription factor that mediates Wnt signaling, is expressed in the distal tip ectoderm [104, 106] and appears to direct dorsal signals to form the nail. In mice with a reduction in Sp8 levels, dorsal dimelia forms (Haro et al., [107]). The distal tip mesoderm also expresses Bambi, a Bmp inhibitor, and Msx1, a transcription factor that is thought to provide regenerative competency to fingertips [104, 108, 109].

Interdigital Cell Death

In the interdigit mesenchyme, BMP signaling also induces cell apoptosis, in part, by repressing Fgf expression in the overlying ectoderm [110]. RA also appears to play a principal role in regulating interdigital cell death. *Rdh10* knockout mice, which fail to convert precursors to RA, show interdigital webbing and a reduction in the expression of *Bmp7* [111]. RA beads are capable of inducing *Bmp* expression and cell death when implanted in the interdigit regions [112]. Weatherbee and coworkers have also suggested that levels of Gremlin, an Shh-regulated factor that inhibits Bmps, correlates with the degree of webbing across species [113]. Thus, Shh and RA signals may work in concert in the interdigital regions to signal digit morphology and interdigital cell death.

Limb Differentiation

While the limb is growing and acquiring its overall shape, cells from both ectoderm and mesoderm begin to differentiate into the various tissues required for limb function. The differentiation process is tightly regulated by signaling molecules of the three axes. Although we will discuss the different tissues separately (vessels, muscle, bone, cartilage, and nervous tissue), these processes are occurring concurrently, with several signaling molecules shared across tissues.

Limb Vasculogenesis

Vascularization begins with the transformation of mesenchymal cells into hemangioblasts [114]. Bmp4 signaling induces the expression of *Flk1* (also known as Vegf-receptor 2) [115], the functional marker of hemangioblasts that confers the capacity to respond to vascular endothelial growth factor (Vegf) [116]. Embryos that lack *Flk1* die around day 9 without any vascular development [117, 118]. Hypoxia-inducible factor 1 (HIF1alpha), sensing the local demands for oxygen in the growing tissue, induces *Vegf* [119]. Bmp4 conjointly with Vegf differentiates hemangioblasts into angioblasts (CD31, CD34, Flk1-positive cells), the precursors of vascular tissue [120, 121].

Angioblasts within the developing limb bud are derived from limb mesenchyme and cells that migrate from adjacent somites [122]. In the emerging limb bud, angioblasts aggregate and differentiate into vascular channels to form the primitive capillary plexuses [121, 123, 124] This process, known as vasculogenesis, is under the control of Vegf [125]. New vessels will sprout from these rudimentary vessels in response to local environmental and chemotactic factors, in a process termed angiogenesis. During angiogenesis, Notch-Delta signaling limits the number of sprouting "tip" cells to support directional outgrowth and remodeling [126, 127]. Interestingly, many of the molecules directing angiogenesis are also involved in axonal guidance (Ephrins/Eph receptors, Slit/Robo signaling, Netrins, Semiphorins, etc.) [128]. This may, in part, explain the parallel pathways taken by these tissues to form neurovascular bundles.

Angiogenesis progressively remodels limb vessels from proximal to distal. In addition to Vegf and Notch signaling, Angiopoietin/Tie signaling is involved in this second stage of vessel formation/remodeling [129, 130]. Around Carnegie stage 13 (day 28 post fertilization), remodeling forms a central limb artery (the primitive subclavian artery) that connects with the dorsal aorta (Fig. 1.10a); concurrently, two peripheral veins form to drain into the posterior cardinal system [123, 131]. The endothelial cells from these remodeled vessels secrete platelet-derived growth factor (Pdgf), which recruits smooth muscle cells and pericytes to surround the growing vessels [132]. Arteries and veins differ in the thickness of surrounding smooth muscle and pericytes. In addition, arteries express Ephrin B2, while veins express Eph-B4 receptors [119].

RA plays an inhibitor role in the angiogenesis process [133, 134]. Experiments with mice lacking Cyp26, an RA degrading enzyme, showed an underdeveloped vasculature that did not progress beyond primitive plexuses [133, 134]. The data suggests that RA can have an inhibitory function on the expression of *Flk1* thus halting the development of vessels [133, 134]. Endothelium expresses Cyp26 and may function to limit the presence of RA [Unpublished data, 132] thereby promoting angiogenesis. Alternatively, these early vessels may limit the level of RA accessible to the developing tissues they supply.

Progressive proximal-to-distal remodeling of limb vessels continues as the limb develops with primitive capillary plexuses persisting in the distal limb until about Carnegie stage 19 (post fertilization day 48). By Carnegie stage 21 (post fertilization day 52), the major vessels and general architecture is completed [135, 136]. The vascular network develops arteries, capillaries, and veins. The low pressure venous sys-

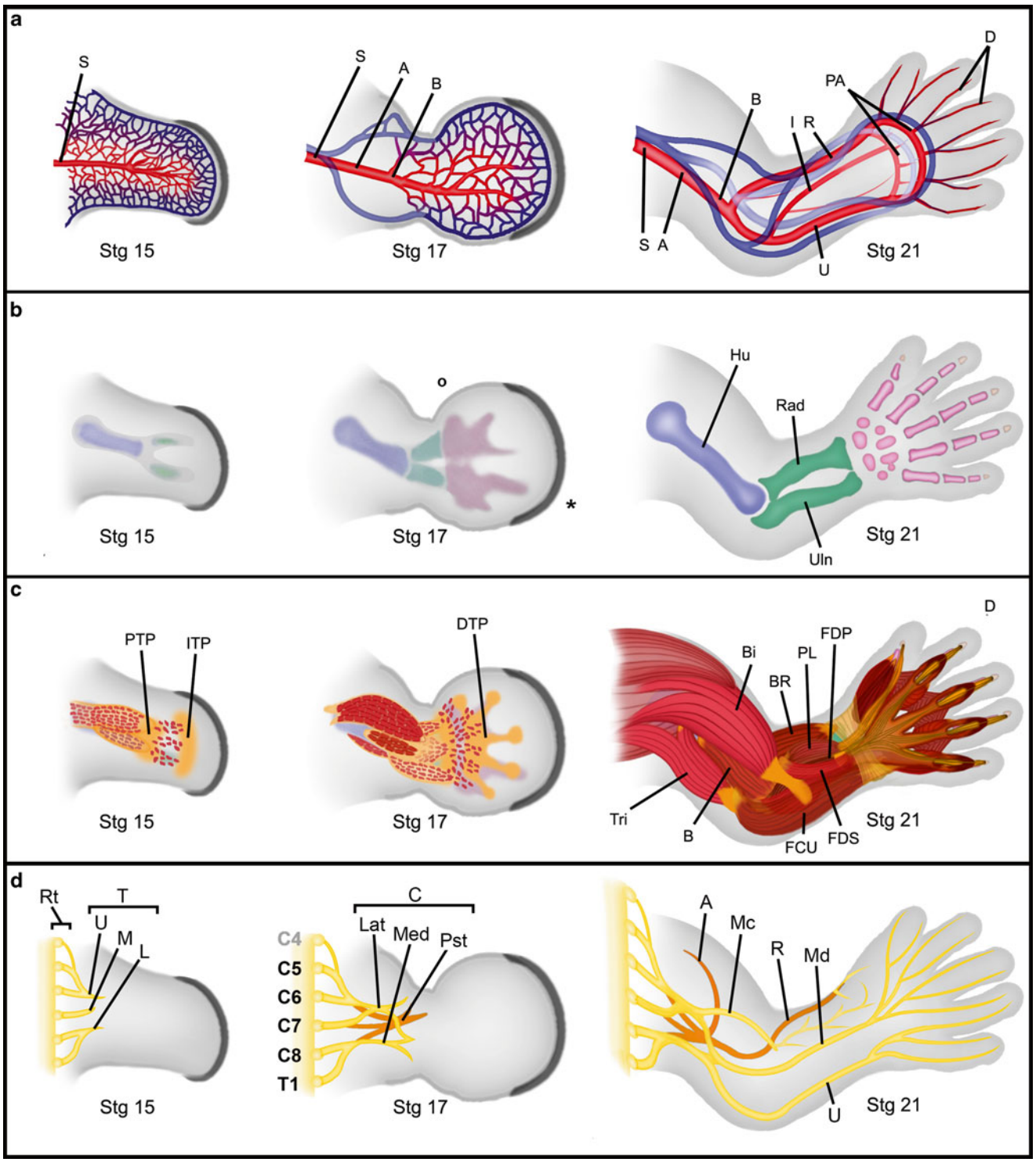

Fig. 1.10 Differentiation of limb tissues. Progressive differentiation of limb tissues from Stage 15 (post fertilization day 35) to stage 21 (day 52 near the end of the embryonic period). (**a**) Vascular differentiation showing the formation and remodeling of the subclavian (S), the axillary (A), the brachial (B), interosseous (I), radial (R), ulnar (U), palmar arch (PA) and digital (D) arteries. (**b**) Progressive skeletal differentiation showing anlagen condensation and definition for the humerus (Hu), radius (Rad), ulna (Uln), carpi and digits. (**c**) Progressive muscle differentiation. Myocyte migration is guided by tendon primoria: First the proximal tendon primordium (PTP) then the intermediate tendon primordium (IPT) and finally the distal tendon primordium (DTP). Secondary myocyte migration and subsequent proliferation within the fascicles defines muscle groups. Triceps (Tri), biceps (Bi), brachialis (B), brachioradialis (BR), flexor carpi ulnaris (FCU), palmaris longus (PL), flexor digitorum superficialis (FDS), and flexor digitorum profundus (FDP). d) Progressive differentiation of limb nerves. The nerve roots (Rt) from cranial 4 through thoracic nerve 1 coalesce to form the upper (U), the middle (M) and lower (L) nerve trunks (T) as they enter the limb bud. Further rearrangements define the lateral (Lat), median (Med), and posterior (Pst) cords (C). As the muscles differentiate and require innervation, major nerves are formed – axillary (A), musculocutaneous (Mc), radial (R), median (Md) and ulnar (U). (Modified from Tonkin and Oberg, 2012) [198]. Courtesy of K.C. Oberg and Loma Linda University

tem is not able to collect all of the fluid distributed to the tissues by the higher pressured arterial system; therefore, a second low pressure vascular system, the lymphatics, forms. The lymphatic vessels also arise from angioblasts that are derived from LPM and somites [122]. Although a unique homeodomain transcription factor, Prox1, distinguishes lymphatics from arterial or venous vessels, the same signaling molecules that direct artery and vein formation likewise appear to control lymphatic vascular development [119].

Limb Skeletogenesis

The limb skeleton is derived from LPM and its development can be described in two steps: (1) chondrogenesis, the process of mesenchymal condensation and chondrocyte differentiation to form endochondral anlagen; and (2) endochondral ossification, the progressive transformation of the cartilage anlagen into the bones of the growing limb. The formation of joints is a related but separate process.

The first indication of chondrogenesis is the up-regulation of Sox9, a high-mobility group transcription factor, in chondrogenic precursors [137]. Sox9 is necessary for skeletogenesis; the lack of Sox9 in animal models results in the complete absence of cartilage and bone, culminating in limb regression [138]. However, Sox9 alone is not sufficient for chondrocyte differentiation. Additional Sox transcription factors (Sox5 and Sox6) are also needed for chondrocyte maturation, i.e., type II collagen production and chondrocyte hypertrophy [139, 140].

Bmp signaling also plays a role in the condensation of cartilaginous anlagen. Studies using constitutively activated and dominant-negative constructs in chicks show that signaling through Bmp receptor 1B (BMPR-1B) is necessary and sufficient to induce cartilage condensation [141]. The induction of Noggin, a potent inhibitor of BMPs, in the limb bud results in the complete absence of mesenchymal condensation [142]. Similarly in mice, knock-out of Bmp receptors 1a and 1b (*BmpR1a*, *BmpR1b*) impairs chondrocyte differentiation and Sox5/6/9 expression [143].

The ablation of individual Bmp proteins instead of their receptors does not prevent chondrogenesis in mice but rather delays the process [70]. This finding suggests that Bmps have a redundant function in chondrogenesis and that a threshold level of Bmp is needed to trigger the induction of Sox 5/6/9 and promote anlagen condensation. Despite the delay in cartilage condensation, individual Bmp knock-out mice exhibit normal endochondral ossification [70] (for a full review of the role of Bmp in skeletogenesis and embryonic development see [144]).

In contrast to Bmp, RA limits the expression and activity of *Sox9* [145, 146]. Experiments with *Cyp26b1* knock-out mice demonstrate impaired RA clearance. The elevated level of RA in the limb arrests or restricts cells to a pre-chondrocytic state and aborts cartilage formation and skeletal progression [147]. Interestingly, Bmp signaling counters this activity by inhibiting *Raldh2*, a gene that encodes for an RA synthesizing enzyme [148]. Thus, Bmps utilize direct and indirect pathways to promote chondrogenesis.

As with other aspects of limb development, chondrogenesis also progresses in a proximal-to-distal fashion. By Carnegie stage 15 (35 days post fertilization), the humerus, radius, and ulna anlagen are evident as a "Y"-shaped condensation (see Fig. 1.10b) [149]. During the next week of gestation (post fertilization days 36–42), condensations form within the handplate. A consistent order of digital condensations in vertebrates has been demonstrated with digit 4 forming first [150, 151] followed by digit 2, digit 5, digit 3, and finally the thumb or digit 1 [82]. Forming last appears to have put the thumb at increased risk, being the most common digit disrupted in malformation syndromes [97]. By Carnegie stage 21, the cartilaginous pattern is established.

Endochondral ossification is mediated in large part by the Runx2 transcription factor that differentiates precursors into osteoblasts and promotes chondrocyte hypertrophy [152]. In addition, Sp7 (also called Osterix), another specificity protein transcription factor, mediates osteocyte maturation, collagen I production and bone matrix deposition [153]. Sp7 works in concert with another transcription factor, ATF4, to maintain osteocyte function [154]. The ossification of long bones is also characterized by an epiphyseal plate that forms between the diaphysis (shaft) and epiphysis (ends). The epiphyseal plate is a growth center responsible for longitudinal growth. At the epiphyseal plate, cartilage proliferation forms regular columns of chondrocytes. These chondrocytes undergo hypertrophy, maturation, and apoptosis with subsequent ossification. These steps are tightly regulated by Runx2, Twist1, Ihh (and Gli3), Vegf, BMP, and FGF signaling [155].

Endochondral ossification transforms the cartilage models into bone. Primary ossification begins as a collar around the diaphyses of all limb long bones except the distal phalanges. Ossification in distal phalanges starts at the distal tip then progresses proximally over the cartilaginous model [104]. There is a consistent sequence to the formation of primary ossification centers in the upper limb. The first anlagen to begin ossification is the humerus (Carnegie stage 23, post fertilization day 56 or 8 weeks gestation), followed by the radius, ulna, distal phalanges, metacarpals, proximal phalanges, and finally middle phalanges by 10 weeks post fertilization [156]. Notably, George L. Steeter, the embryologist entrusted with characterizing the Carnegie collection of human gestations in the 1940s, regarded humeral ossification as the *sine qua non* of the beginning of the fetal period. Thus, the initiation of limb long bone ossification with the formation of primary ossification centers is a fetal endeavor.

Ossification of carpal bones does not start until around the time of birth [157]. The initiation of carpal ossification also follows a typical sequence beginning with the capitate and

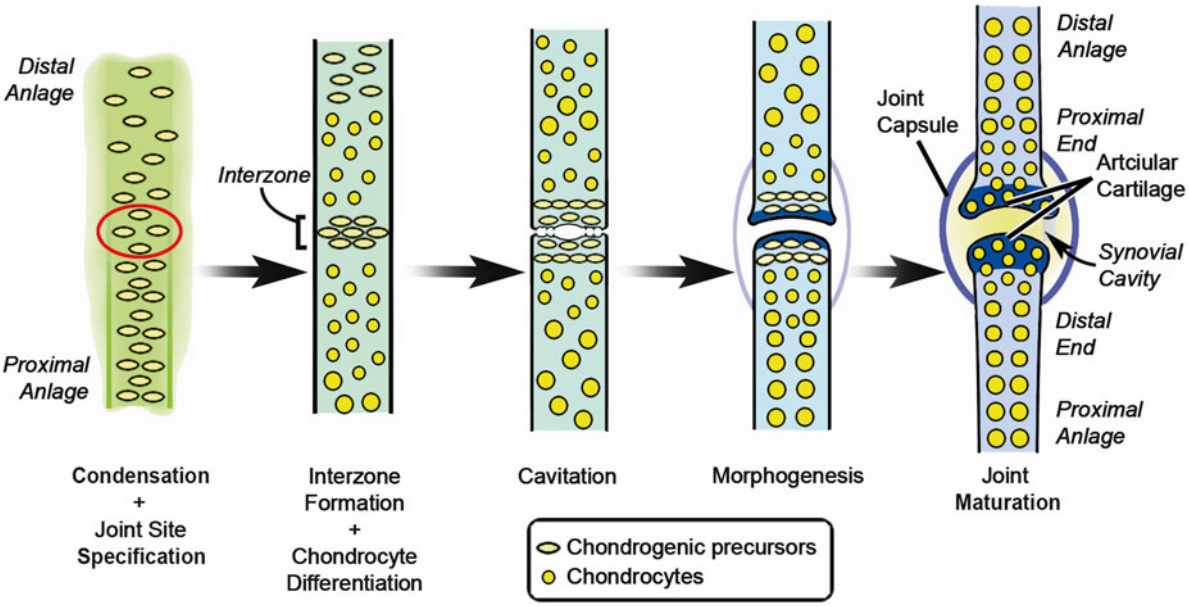

Fig. 1.11 Joint formation. Transformation of a presumptive joint in cartilage anlagen to a joint with synovial cavity and capsule (Image adapted from Pacifici et al., 2005) [164]. Courtesy of K.C. Oberg and Loma Linda University

hamate (the ulnar aspect of the distal row) and ending with the trapezium, trapezoid (the radial aspect of the distal row), and the scaphoid (the radial aspect of the proximal row) [157]. Formation of secondary ossification centers within the epiphyses of the long bones also occurs postnatally. The characteristic pattern of hand and wrist ossification is a useful tool in assessing skeletal maturity in children. Prior to puberty, a sex-related difference is evident in hand and wrist ossification; in girls, formation of primary ossification centers is completed at around 6 years of age, whereas in boys, it is completed around 8 years of age [157].

The expression of the distal Hoxa transcription factors, Hoxa10, Hoxa11, and Hoxa13, correlates with the stylopod (arm), the zeugopod (forearm), and autopod (hand), respectively [76]. Synovial joints form within the developing skeletal anlagen at the boundaries between these three skeletal segments. Morphologically, a joint passes through three stages (Fig. 1.11): (1) interzone formation, with condensation of a cell dense region of flattened cells called the interzone; (2) cavitation, the formation of a gap separating the two skeletal elements; and (3) morphogenesis, the process of forming complementary articular cartilage-lined surfaces to facilitate movement. Wnt14 is expressed in the presumptive joint and up-regulates Gdf5 prior to interzone formation [158]. Gdf5 becomes tightly restricted to the interzone as it forms and promotes subsequent joint formation [159]. Centrally the interzone begins to cavitate, becomes hypocellular, and accumulates hyaluronan [160, 161]. Although joint-related muscular contractions are not needed for interzone formation, they are essential for proper cavitation to occur [162]. Integrated axis-related patterning pathways and cell movement work together to form complementary cartilage-lined surfaces on the opposing skeletal ends for appropriate articulation [163, 164]. Concurrently, mesoderm surrounding the developing joint condenses, forming fortifying ligaments and the joint capsule [165, 166].

Limb Myogenesis

Formation of the upper limb musculature is an integrated process involving tendons, myocytes, and nerves. Disruption of any one of these structures results in muscle abnormalities [167]. The arrangement of tendons and their sites of bony attachment establish the framework within which muscles will develop (see Fig. 1.10c). The tendon primordia develop from limb mesenchyme. The first indication of tendon formation is the expression of Scleraxis (Scx), a tendon-specific transcription factor in precursor tenocytes [168]. Subsequently, the cells express the extracellular matrix protein tenascin [169].

Three dorsal–ventral pairs of tendon primordia progressively develop within each limb segment [170]. The tendon primordia, which includes connective tissue cells that will encase and direct the developing myocytes, forms under the influence of axis-related signals and initially is independent from the influence of migrating myocytes [171]. For example, Wnt7a from the dorsal ectoderm regulates dorsal tendon formation and mice that lack *En-1*, the transcription factor that limits Wnt7a expression to the dorsal ectoderm, develop a symmetrical bi-dorsal phenotype, i.e., dorsal or extensor tendons for both the dorsal and "ventral" aspects of the limb [62, 65]. However, muscle interaction is an absolute require-

ment for maintenance of the tendon primordia and the final muscle arrangement; in muscle deficient limbs, the tendons form but then degenerate [170].

Muscle undergoes progressive and somewhat overlapping phases of development [172]: (1) an embryonic phase with development of primary mononuclear fibers from migrating myoblasts; (2) a fetal/neonatal phase generating secondary multinucleate fibers from migrating myoblasts; and (3) an adult phase that contributes multinucleated fibers derived from satellite cells.

The first marker of limb-related myocyte differentiation during the embryonic phase of myogenesis is the expression of Pax3, a pair-ruled homeodomain transcription factor, in the dorsolateral cells of the dermomyotome in limb-associated somites [173–175]. Subsequently, the Pax3-positive cells will delaminate and migrate into the developing limb bud. *Pax3* knock-out mice show a loss of limb musculature and a loss of cell movements away from the somite [173, 176].

Delamination and migration are also dependent upon scatter factor/hepatocyte growth factor (Sf/Hgf) secreted from the developing limb bud mesenchyme and the corresponding expression of the Sf/Hgf receptor (c-met) in the myocyte precursors [177–180]. Pax3 regulates the expression of *c-met* in myocytes [181], while AER-associated Fgfs via Fgfr4 signaling control *Sf/Hgf* expression and thus the migratory routes of myocytes [180]. Mice deficient in *c-met* or *Hgf* expression lack migration and show a complete absence of limb musculature [178, 182].

As the myocyte precursors migrate into the limb bud, they split into dorsal and ventral precursors. Lbx1, a homeodomain transcription factor expressed in dorsal myocyte precursors, mediates this segregation. Disruption of *Lbx1* disrupts dorsal muscle migration without significantly affecting the migration of ventral myocytes [183].

AER-related Fgfs regulate the expression of SF/Hgf within the limb mesoderm thereby controlling the migration of myocytes as they infiltrate tendon primordia to arrive at their final destination [180]. Within the limb bud, myocyte precursors begin to express *MyoD* and *Myf5*, committing them to a myocyte fate [184]. Activation of these myocyte-specific genes is also thought to depend on axis-related signal molecules, such as Wnt7a and Shh [174, 180]. The myocytes elongate and form primary mononuclear muscle fibers.

Progressive proximal-to-distal differentiation also occurs during myogenesis (see Fig. 1.10c). As myocyte precursors extend into the distal primordial tendons, a second wave of myocyte precursors migrates into the proximal limb. These myocyte precursors express Pax7 in addition to Pax3. Some of these precursors will coalesce around primary myofibers and fuse to form secondary multinucleated myofibers [185]. In addition, a population will remain in a precursor state at the periphery as a satellite cell [186]. Adult multinucleated muscle fibers are derived from satellite cells. It is during secondary or fetal myogenesis that motor endplates form and neuromuscular communication begins.

Limb Innervation

Innervation of the limb follows myocyte migration (see Fig. 1.10d). The axons of both motor and sensory neurons from the limb-associated spinal cord aggregate at the proximal limb boundary, forming several thick fascicles. These fascicles differentiate into the upper, middle, and lower trunks of the brachial plexus [187]. The nerve fascicles enter the limb then subdivide into dorsal and ventral branches. The dorsal branches coalesce to form the posterior cord. The upper and middle regions of the ventral branches join to form the lateral cord and the lower branch continues as medial cord. The cords then divide into the terminal branches of mixed motor and sensory axons. These branches follow a predictable pattern within the limb bud that appear to be controlled by variations in the extracellular matrix [188–190]. The initial entrance and distribution of the terminal branches within the limb do not appear to require signals from the final target tissue. However, for terminal sensory branching, the presence of skin is required [191]. Similarly, for fine targeted branching of motor nerves, differentiating muscle bundles are required [192].

The molecular control of axonal guidance and tissue targeting begins prior to axonal outgrowth during motor neuron differentiation. Shh secreted from the notochord and the floor plate of the spinal cord induces motor neuron and pancreas *homeobox1* (*Mnx1*, previously called *Hb9*), which encodes a transcription factor that transforms the neuroepithelium into motor neurons [193]. Hox transcription factors expressed within the spinal cord organize motor neurons destined for the upper limb into the lateral motor column (LMC), which is also demarcated by the expression of Islet1 and Islet2 (Isl1/Isl2) lim homeodomain transcription factors. The expression of *Raldh2*, and thus the production of RA, within the lateral LMC induces the expression of lim homeodomain 1 (Lhx1) transcription factor and inhibits the expression of Isl1, further subdividing the LMC into medial Isl1/Isl2-positive neurons that will project into the ventral limb and lateral Lhx1/Isl2-positive neurons that extend into the dorsal limb [194].

A second phase of complex Hox transcription factor expression coupled with the expression of forkhead box P1 (FoxP1) transcription factor is thought to convey axon targeting information to specific partner muscles within the limb defined by axis-related cues [195]. A complex interplay of Ephrins and Eph receptors is involved in the regulation of branching and axonal guidance (see Kao et al. [195] for a comprehensive review). Finally, at the target site, Etv4

Table 1.1 Comparison of the Swanson's and OMT classification schemes

I. Failure of formation of parts/arrest of development	I. Malformations
– Transverse deficiencies	A. Abnormal axis formation/differentiation—entire upper limb
– Longitudinal deficiencies	1. Proximal–distal axis
II. Failure of separation or differentiation of parts	2. Radial–ulnar (anterior-posterior) axis
– Soft tissue deficiency	3. Dorsal–ventral axis
– Skeletal deficiency	4. Unspecified axis
III. Duplication	B. Abnormal axis formation/differentiation—hand plate
– Radial polydactyly	1. Proximal–distal axis
– Central polydactyly	2. Radial–ulnar (anterior-posterior) axis
– Ulnar polydactyly	3. Dorsal–ventral axis
– Mirror hand/Ulnar dimelia	4. Unspecified axis
IV. Overgrowth	II. Deformations
– Hemihypertrophy	A. Constriction ring sequence
– Macrodactyly	B. Trigger digits
V. Undergrowth	C. Not otherwise specified
– Hypoplastic hand	III. Dysplasias
– Brachymetacarpia	A. Hypertrophy
– Brachydactyly	1. Whole limb
VI. Constriction band syndrome	2. Partial limb
VII. Generalized skeletal disorder	B. Tumorous conditions
	1. Vascular
	2. Neurological
	3. Connective tissue
	4. Skeletal
	IV. Syndromes

transcription factors are required to promote the axonal arborization needed for terminal neuromuscular innervation [196].

Dysmorphogenesis and Classification

Congenital upper limb anomaly designations are typically based on appearance. We readily understand the terms such as polydactyly, syndactyly, or radial club hand. However, these terms often fail to inform us of the prognosis, approach to treatment, or the etiology. Many equate congenital upper limb malformations with abnormalities of the skeleton, but disruption of any aspect of limb development can lead to dysmorphology including vascular and neuromuscular differentiation. Classification provides a mechanism to organize dysmorphologies into categories that describe one or more aspects of these anomalies. Ideally, a classification for upper limb anomalies would incorporate the etiologic basis, provide insight into prognosis, and guide treatment [197]. Furthermore, it should provide a universal language for discussion across disciplines regarding epidemiology, treatment, and research [198].

A number of classification schemes have been proposed to organize the known spectrum of upper limb anomalies. Probably the earliest recorded classification system was in 1829 by Isidore Saint-Hilaire who initially described anomalies simply as mild or severe [199]. He subsequently focused on what was missing, coining the terms ectromelia (limb absence), phocomelia (missing limb segments), and hemimelia (missing limb parts) [200]. In 1895, Kümmel described upper limb anomalies in terms of defects (deficiencies), adhesions (fusions), or superior numbers (duplications).

Swanson proposed a new classification scheme in 1964 [201]. Swanson's scheme was geared to hand surgeons and was considered to be an anatomic and clinical classification that indicated the type of primary embryonic damage [202]. While in the emerging field of clinical genetics, Temtamy had proposed a classification that focused on the genetic basis of malformation [202–204]. A modified version of Swanson's classification, subsequently adopted by the International Federation of Societies for Surgery of the Hand (IFSSH) in 1974, categorized limb anomalies based on failed formation, failed differentiation, duplication, overgrowth, undergrowth, constriction bands, and generalized skeletal anomalies (Table 1.1) [205]. This same year, Kelikian reviewed a number of the classifications schemes that had been proposed and insightfully concluded that our knowledge was still insufficient to formulate a "comprehensive classification" [206].

Nevertheless, the modified Swanson's classification served as the primary basis for scientific communication and discussion for upper limb anomalies among hand surgeons for more than 40 years [197]. With time it was recognized

that complex disorders were difficult or impossible to classify within this scheme, prompting a number of authors to suggest modifications [207, 208].

Increased knowledge of the molecular basis of limb development from clinical genetics and developmental biology has also challenged the utility of many of the categories in indicating the underlying etiology. For example, altered Shh expression along the radial–ulnar axis can cause ulnar deficiency, triphalangeal thumb, and ulnar dimelia, but these three conditions are listed separately in different categories with no mechanism to demonstrate that all three conditions are part of the same molecular pathway [197, 208, 209]. Mounting evidence regarding the etiology of cleft hand prompted the Japanese Society for Surgery of the Hand to add two additional groups: Group IV, abnormal induction of digital rays (thereby shifting the subsequent groups to V through VIII) and Group IX, unclassifiable cases [210]. However, this modification does not address the need to incorporate genetic etiologic information into other conditions. Our increased knowledge requires a more comprehensive classification system.

In 2010, a new classification scheme was proposed that combined anatomic and genetic information [209] (see Table 1.1). To facilitate communication, the authors, Drs Oberg, Manske, and Tonkin, used the general headings "Malformation, Deformation and Dysplasia," terms well established and used by dysmorphologists, clinical geneticists, and developmental biologists. The headings and sub-

Table 1.2 The new IFSSH (OMT) extended classification of congenital hand and upper limb anomalies

I. Malformations
A. Abnormal axis formation/differentiation—entire upper limb
1. Proximal–distal axis
(i) Brachymelia with brachydactyly
(ii) Symbrachydactyly
(a) Poland syndrome
(b) Whole limb excluding Poland syndrome
(iii) Transverse deficiency
(a) Amelia
(b) Clavicular/scapular
(c) Humeral (above elbow)
(d) Forearm (below elbow)
(e) Wrist (carpals absent/at level of proximal carpals/at level of distal carpals) (with forearm/arm involvement)
(f) Metacarpal (with forearm/arm involvement)
(g) Phalangeal (proximal/middle/distal) (with forearm/arm involvement)
(iv) Intersegmental deficiency
(a) Proximal (humeral—rhizomelic)
(b) Distal (forearm—mesomelic)
(c) Total (Phocomelia)
(v) Whole limb duplication/triplication
2. Radial–ulnar (anterior-posterior) axis
(i) Radial longitudinal deficiency—Thumb hypoplasia (with proximal limb involvement)
(ii) Ulnar longitudinal deficiency
(iii) Ulnar dimelia
(iv) Radioulnar synostosis
(v) Congenital dislocation of the radial head
(vi) Humeroradial synostosis—Elbow ankyloses
3. Dorsal–ventral axis
(i) Ventral dimelia
(a) Fuhrmann/Al-Awadi/Raas-Rothschild syndromes
(b) Nail–Patella syndrome
(ii) Absent/hypoplastic extensor/flexor muscles
4. Unspecified axis
(i) Shoulder
(a) Undescended (Sprengel)
(b) Abnormal shoulder muscles
(c) Not otherwise specified
(ii) Arthrogryposis

(continued)

Table 1.2 (continued)

- B. Abnormal axis formation/differentiation—hand plate
  - 1. Proximal–distal axis
    - (i) Brachydactyly (no forearm/arm involvement)
    - (ii) Symbrachydactyly (no forearm/arm involvement)
    - (iii) Transverse deficiency (no forearm/arm involvement)
      - (a) Wrist (carpals absent/at level of proximal carpals/at level of distal carpals)
      - (b) Metacarpal
      - (c) Phalangeal (proximal/middle/distal)
  - 2. Radial–ulnar (anterior-posterior) axis
    - (i) Radial deficiency (thumb—no forearm/arm involvement)
    - (ii) Ulnar deficiency (no forearm/arm involvement)
    - (iii) Radial polydactyly
    - (iv) Triphalangeal thumb
    - (v) Ulnar dimelia (mirror hand—no forearm/arm involvement)
    - (vi) Ulnar polydactyly
  - 3. Dorsal–ventral axis
    - (i) Dorsal dimelia (palmar nail)
    - (ii) Ventral (palmar) dimelia (including hypoplastic/aplastic nail)
  - 4. Unspecified axis
    - (i) Soft tissue
      - (a) Syndactyly
      - (b) Camptodactyly
      - (c) Thumb in palm deformity
      - (d) Distal arthrogryposis
    - (ii) Skeletal deficiency
      - (a) Clinodactyly
      - (b) Kirner's deformity
      - (c) Synostosis/symphalangism (carpal/metacarpal/phalangeal)
    - (iii) Complex
      - (a) Complex syndactyly
      - (b) Synpolydactyly—central
      - (c) Cleft hand
      - (d) Apert hand
      - (e) Not otherwise specified

II. Deformations
- A. Constriction ring sequence
- B. Trigger digits
- C. Not otherwise specified

III. Dysplasias
- A. Hypertrophy
  - 1. Whole limb
    - (i) Hemihypertrophy
    - (ii) Aberrant flexor/extensor/intrinsic muscle
  - 2. Partial limb
    - (i) Macrodactyly
    - (ii) Aberrant intrinsic muscles of hand
- B. Tumorous conditions
  - 1. Vascular
    - (i) Hemangioma
    - (ii) Malformation
    - (iii) Others
  - 2. Neurological
    - (i) Neurofibromatosis
    - (ii) Others

(continued)

Table 1.2 (continued)

3. Connective tissue
(i) Juvenile aponeurotic fibroma
(ii) Infantile digital fibroma
(iii) Others
4. Skeletal
(i) Osteochondromatosis
(ii) Enchondromatosis
(iii) Fibrous dysplasia
(iv) Epiphyseal abnormalities
(v) Others
IV. Syndromes[a]
A. Specified
1. Acrofacial Dysostosis 1 (Nager type)
2. Apert
3. Al-Awadi/Raas-Rothschild/Schinzel phocomelia
4. Baller-Gerold
5. Bardet-Biedl Carpenter
6. Catel-Manzke
7. Constriction band (Amniotic Band Sequence)
8. Cornelia de Lange (types 1-5)
9. Crouzon
10. Down
11. Ectrodactyly-Ectodermal Dysplasia-Clefting
12. Fanconi Pancytopenia
13. Fuhrmann
14. Goltz
15. Gorlin
16. Greig Cephalopolysyndactyly
17. Hajdu-Cheney
18. Hemifacial Microsomia (Goldenhar syndrome)
19. Holt-Oram
20. Lacrimoauriculodentodigital (Levy-Hollister)
21. Larsen
22. Leri-Weill Dyschondrosteosis
23. Moebius sequence
24. Multiple Synostoses
25. Nail-Patella
26. Noonan
27. Oculodentodigital dysplasia
28. Orofacialdigital
29. Otopalataldigital
30. Pallister-Hall
31. Pfeiffer
32. Poland
33. Proteus
34. Roberts-SC Phocomelia
35. Rothmund-Thomson
36. Rubinstein-Taybi
37. Saethre-Chotzen
38. Thrombocytopenia Absent Radius
39. Townes-Brock
40. Trichorhinophalangeal (types 1-3)
41. Ulnar-Mammary
42. VACTERLS association
B. Others

[a]The specified list of syndromes are those considered most relevant; however, many other syndromes have a limb component and are "B. Others"

headings indicate not only the altered morphology but also the disrupted molecular pathways identified by clinical genetics. The "OMT" classification scheme has undergone critical evaluation by a group of international hand surgeons (the Congenital Hand Anomalies Study Group, or CHASG) and its capacity/utility to classify upper limb malformations demonstrated [211]. In February of 2014, the OMT classification was adopted by the IFSSH as the recommended classification scheme [212].

Malformations

Malformations are failures of normal development and/or differentiation and are, by far, the most common form of upper limb anomaly [213]. Malformations are subdivided into "Entire upper limb" and "Handplate" based on basic limb development and evolutionary patterning. Although the three basic axes of development are in play for the handplate as well as the entire limb, the handplate recruits a number of additional molecules/molecular cascades to pattern the increased complexity of the hand. Correspondingly, the handplate has more evolutionary variation and more targets for dysmorphogenesis [97]. This has been corroborated by a recent epidemiological study of congenital hand anomalies in Stockholm, Sweden, using this new classification scheme, with 356 of the 429 malformations being classified as handplate anomalies (and only 73 as entire upper limb) [213].

Malformations are further subdivided by the primary axis disrupted (Table 1.2). Using the example above, ulnar longitudinal deficiency (ULD), ulnar dimelia, and triphalangeal thumb are all subclassified as disorders of the radial–ulnar axis. ULD and ulnar dimelia are both disorders of the entire upper limb, while triphalangeal thumb is a disorder limited to the handplate. A category entitled "Unspecified axis" is included for entities that do not have a known axis-related nature (e.g., syndactyly) or the suspected axis-related nature is not yet characterized (e.g., clinodactyly).

Deformations

Deformations occur after normal development and differentiation; from an intervention standpoint, there is a better chance that normal structures will still be present. Dysmorphologists also speak of disruption, which is a breakdown of normal tissues, often vascular. For the purposes of congenital upper limb anomalies, both disruption and deformation are changes that occur after development so are collectively included under the heading "Deformation." The classic example is constriction ring sequence (also called amniotic band sequence), which can result in deformed or disrupted tissues. No axis-related subclassification is used because deformations occur after and exogenous to patterned development.

Dysplasias

Dysplasias are abnormalities of development and/or differentiation of isolated tissues common to the limb such as vascular, neural, or skeletal. Dysplasias can disrupt normal development (malformation) and/or cause progressive deformation.

Syndromes

It is not possible to list all of the syndromes that have a limb anomaly as a component. For example, there are over 110 syndromes with thumb hypoplasia or aplasia as a feature [97]. In the following chapter (Chap. 2), Drs. Laub and Burke will review syndromes that have an upper limb anomaly as a primary feature.

In summary, this new classification scheme combining anatomic and genetic information about congenital anomalies has been introduced to the IFSSH member societies by the IFSSH Congenital Committee [214]. Although our knowledge is still insufficient, hopefully we are a step closer to a comprehensive classification system.

Acknowledgements The authors would like to thank Charmaine Pira for suggestions, insight, and careful review of this manuscript.

References

1. O'Rahilly R, Muller F. Developmental stages in human embryos. Washington, DC: Carnegie Institution of Washington; 1987.
2. Tickle C. Embryology. In: AKS Gupta (Ed.), *The growing hand: diagnosis and management of the upper extremity in children*. Sheker LR. London: CV Mosby; 2000;25–32.
3. Cohn MJ, Tickle C. Developmental basis of limblessness and axial patterning in snakes. Nature. 1999;399(6735):474–9.
4. Burke AC, Nelson CE, Morgan BA, Tabin C. Hox genes and the evolution of vertebrate axial morphology. Development. 1995;121(2):333–46.
5. Searls RL, Janners MY. The initiation of limb bud outgrowth in the embryonic chick. Dev Biol. 1971;24(2):198–213.
6. Kawakami Y, Capdevila J, Buscher D, Itoh T, Rodriguez Esteban C, Izpisua Belmonte JC. WNT signals control FGF-dependent limb initiation and AER induction in the chick embryo. Cell. 2001;104(6):891–900.
7. Ohuchi H, Nakagawa T, Yamamoto A, Araga A, Ohata T, Ishimaru Y, Yoshioka H, Kuwana T, Nohno T, Yamasaki M, et al. The mesenchymal factor, FGF10, initiates and maintains the outgrowth of the chick limb bud through interaction with FGF8, an apical ectodermal factor. Development. 1997;124(11):2235–44.
8. Minguillon C, Del Buono J, Logan MP. Tbx5 and Tbx4 are not sufficient to determine limb-specific morphologies but have com-

mon roles in initiating limb outgrowth. Dev Cell. 2005;8(1):75–84.
9. Minguillon C, Nishimoto S, Wood S, Vendrell E, Gibson-Brown JJ, Logan MP. Hox genes regulate the onset of Tbx5 expression in the forelimb. Development. 2012;139(17):3180–8.
10. Pizette S, Abate-Shen C, Niswander L. BMP controls proximodistal outgrowth, via induction of the apical ectodermal ridge, and dorsoventral patterning in the vertebrate limb. Development. 2001;128(22):4463–74.
11. Soshnikova N, Zechner D, Huelsken J, Mishina Y, Behringer RR, Taketo MM, Crenshaw III EB, Birchmeier W. Genetic interaction between Wnt/beta-catenin and BMP receptor signaling during formation of the AER and the dorsal-ventral axis in the limb. Genes Dev. 2003;17(16):1963–8.
12. Barrow JR, Thomas KR, Boussadia-Zahui O, Moore R, Kemler R, Capecchi MR, McMahon AP. Ectodermal Wnt3/beta-catenin signaling is required for the establishment and maintenance of the apical ectodermal ridge. Genes Dev. 2003;17(3):394–409.
13. Abu-Abed S, Dolle P, Metzger D, Beckett B, Chambon P, Petkovich M. The retinoic acid-metabolizing enzyme, CYP26A1, is essential for normal hindbrain patterning, vertebral identity, and development of posterior structures. Genes Dev. 2001;15(2):226–40.
14. Hogan BL, Thaller C, Eichele G. Evidence that Hensen's node is a site of retinoic acid synthesis. Nature. 1992;359(6392):237–41.
15. Niederreither K, McCaffery P, Drager UC, Chambon P, Dolle P. Restricted expression and retinoic acid-induced downregulation of the retinaldehyde dehydrogenase type 2 (RALDH-2) gene during mouse development. Mech Dev. 1997;62(1):67–78.
16. Cunningham TJ, Zhao X, Sandell LL, Evans SM, Trainor PA, Duester G. Antagonism between retinoic acid and fibroblast growth factor signaling during limb development. Cell Rep. 2013;3(5):1503–11.
17. Zhao X, Sirbu IO, Mic FA, Molotkova N, Molotkov A, Kumar S, Duester G. Retinoic acid promotes limb induction through effects on body axis extension but is unnecessary for limb patterning. Curr Biol. 2009;19(12):1050–7.
18. Kessel M, Gruss P. Homeotic transformations of murine vertebrae and concomitant alteration of Hox codes induced by retinoic acid. Cell. 1991;67(1):89–104.
19. Deschamps J. Ancestral and recently recruited global control of the Hox genes in development. Curr Opin Genet Dev. 2007;17(5):422–7.
20. Wolpert L. Positional information and the spatial pattern of cellular differentiation. J Theor Biol. 1969;25(1):1–47.
21. Fallon JF, Kelley RO. Ultrastruct analysis of the apical ectodermal ridge during vertebrate limb morphogenesis. II. Gap junctions as distinctive ridge structures common to birds and mammals. J Embryol Exp Morphol. 1977;41:223–32.
22. Summerbell D, Lewis JH. Time, place and positional value in the chick limb-bud. J Embryol Exp Morphol. 1975;33(3):621–43.
23. Chiang C, Litingtung Y, Harris MP, Simandl BK, Li Y, Beachy PA, Fallon JF. Manifestation of the limb prepattern: limb development in the absence of sonic hedgehog function. Dev Biol. 2001;236(2):421–35.
24. Ros MA, Dahn RD, Fernandez-Teran M, Rashka K, Caruccio NC, Hasso SM, Bitgood JJ, Lancman JJ, Fallon JF. The chick oligozeugodactyly (ozd) mutant lacks sonic hedgehog function in the limb. Development. 2003;130(3):527–37.
25. MacCabe JA, Errick J, Saunders Jr JW. Ectodermal control of the dorsoventral axis in the leg bud of the chick embryo. Dev Biol. 1974;39(1):69–82.
26. Lewandoski M, Sun X, Martin GR. Fgf8 signalling from the AER is essential for normal limb development. Nat Genet. 2000;26(4):460–3.
27. Fernandez-Teran M, Ros MA. The Apical Ectodermal Ridge: morphological aspects and signaling pathways. Int J Dev Biol. 2008;52(7):857–71.
28. Niswander L, Tickle C, Vogel A, Booth I, Martin GR. FGF-4 replaces the apical ectodermal ridge and directs outgrowth and patterning of the limb. Cell. 1993;75(3):579–87.
29. Fallon JF, Lopez A, Ros MA, Savage MP, Olwin BB, Simandl BK. FGF-2: apical ectodermal ridge growth signal for chick limb development. Science. 1994;264(5155):104–7.
30. Mariani FV, Ahn CP, Martin GR. Genetic evidence that FGFs have an instructive role in limb proximal-distal patterning. Nature. 2008;453(7193):401–5.
31. Sun X, Lewandoski M, Meyers EN, Liu YH, Maxson Jr RE, Martin GR. Conditional inactivation of Fgf4 reveals complexity of signalling during limb bud development. Nat Genet. 2000;25(1):83–6.
32. Sun X, Mariani FV, Martin GR. Functions of FGF signalling from the apical ectodermal ridge in limb development. Nature. 2002;418(6897):501–8.
33. Boulet AM, Moon AM, Arenkiel BR, Capecchi MR. The roles of Fgf4 and Fgf8 in limb bud initiation and outgrowth. Dev Biol. 2004;273(2):361–72.
34. Summerbell D, Lewis JH, Wolpert L. Positional information in chick limb morphogenesis. Nature. 1973;244(5417):492–6.
35. Summerbell D, Wolpert L. Precision of development in chick limb morphogenesis. Nature. 1973;244(5413):228–30.
36. Dudley AT, Ros MA, Tabin CJ. A re-examination of proximodistal patterning during vertebrate limb development. Nature. 2002;418(6897):539–44.
37. Tabin C, Wolpert L. Rethinking the proximodistal axis of the vertebrate limb in the molecular era. Genes Dev. 2007;21(12):1433–42.
38. Rosello-Diez A, Ros MA, Torres M. Diffusible signals, not autonomous mechanisms, determine the main proximodistal limb subdivision. Science. 2011;332(6033):1086–8.
39. Rosello-Diez A, Torres M. Regulative patterning in limb bud transplants is induced by distalizing activity of apical ectodermal ridge signals on host limb cells. Dev Dyn. 2011;240(5):1203–11.
40. Yashiro K, Zhao X, Uehara M, Yamashita K, Nishijima M, Nishino J, Saijoh Y, Sakai Y, Hamada H. Regulation of retinoic acid distribution is required for proximodistal patterning and outgrowth of the developing mouse limb. Dev Cell. 2004;6(3):411–22.
41. Knezevic V, De Santo R, Schughart K, Huffstadt U, Chiang C, Mahon KA, Mackem S. Hoxd-12 differentially affects preaxial and postaxial chondrogenic branches in the limb and regulates Sonic hedgehog in a positive feedback loop. Development. 1997;124(22):4523–36.
42. Saunders JW, Gasseling MT. Ectodermal-mesenchymal interactions in the origin of limb symmetry. In: Fleischmajer R, Billingham RE, editors. Epithelial-mesenchymal interactions. Baltimore: William and Wilkins; 1968. p. 78–97.
43. Tickle C, Summerbell D, Wolpert L. Positional signalling and specification of digits in chick limb morphogenesis. Nature. 1975;254(5497):199–202.
44. Tickle C. Limb regeneration. Am Sci. 1981;69(6):639–46.
45. Tickle C, Lee J, Eichele G. A quantitative analysis of the effect of all-trans-retinoic acid on the pattern of chick wing development. Dev Biol. 1985;109(1):82–95.
46. Tickle C, Crawley A, Farrar J. Retinoic acid application to chick wing buds leads to a dose-dependent reorganization of the apical ectodermal ridge that is mediated by the mesenchyme. Development. 1989;106(4):691–705.
47. Tickle C. Retinoic acid and chick limb bud development. Dev Suppl. 1991;1:113–21.
48. Wanek N, Gardiner DM, Muneoka K, Bryant SV. Conversion by retinoic acid of anterior cells into ZPA cells in the chick wing bud. Nature. 1991;350(6313):81–3.

49. Riddle RD, Johnson RL, Laufer E, Tabin C. Sonic hedgehog mediates the polarizing activity of the ZPA. Cell. 1993;75(7): 1401–16.
50. Kraus P, Fraidenraich D, Loomis CA. Some distal limb structures develop in mice lacking Sonic hedgehog signaling. Mech Dev. 2001;100(1):45–58.
51. Xu B, Wellik DM. Axial Hox9 activity establishes the posterior field in the developing forelimb. Proc Natl Acad Sci U S A. 2011;108(12):4888–91.
52. Zeller R, Lopez-Rios J, Zuniga A. Vertebrate limb bud development: moving towards integrative analysis of organogenesis. Nat Rev Genet. 2009;10(12):845–58.
53. Charitè J, McFadden DG, Olson EN. The bHLH transcription factor dHAND controls Sonic hedgehog expression and establishment of the zone of polarizing activity during limb development. Development. 2000;127(11):2461–70.
54. Capellini TD, Di GG, Salsi V, Brendolan A, Ferretti E, Srivastava D, Zappavigna V, Selleri L. Pbx1/Pbx2 requirement for distal limb patterning is mediated by the hierarchical control of Hox gene spatial distribution and Shh expression. Development. 2006;133(11):2263–73.
55. Zakany J, Kmita M, Duboule D. A dual role for Hox genes in limb anterior-posterior asymmetry. Science. 2004;304(5677):1669–72.
56. Schimmang T, Lemaistre M, Vortkamp A, Ruther U. Expression of the zinc finger gene Gli3 is affected in the morphogenetic mouse mutant extra-toes (Xt). Development. 1992;116(3): 799–804.
57. Hui CC, Joyner AL. A mouse model of greig cephalopolysyndactyly syndrome: the extra-toesJ mutation contains an intragenic deletion of the Gli3 gene. Nat Genet. 1993;3(3):241–6.
58. Litingtung Y, Dahn RD, Li Y, Fallon JF, Chiang C. Shh and Gli3 are dispensable for limb skeleton formation but regulate digit number and identity. Nature. 2002;418(6901):979–83.
59. te Welscher P, Zuniga A, Kuijper S, Drenth T, Goedemans HJ, Meijlink F, Zeller R. Progression of vertebrate limb development through SHH-mediated counteraction of GLI3. Science. 2002;298(5594):827–30.
60. McGlinn E, van Bueren KL, Fiorenza S, Mo R, Poh AM, Forrest A, Soares MB, Bonaldo Mde F, Grimmond S, Hui CC, et al. Pax9 and Jagged1 act downstream of Gli3 in vertebrate limb development. Mech Dev. 2005;122(11):1218–33.
61. Parr BA, McMahon AP. Dorsalizing signal Wnt-7a required for normal polarity of D-V and A-P axes of mouse limb. Nature. 1995;374(6520):350–3.
62. Loomis CA, Harris E, Michaud J, Wurst W, Hanks M, Joyner AL. The mouse Engrailed-1 gene and ventral limb patterning. Nature. 1996;382(6589):360–3.
63. Logan C, Hornbruch A, Campbell I, Lumsden A. The role of Engrailed in establishing the dorsoventral axis of the chick limb. Development. 1997;124(12):2317–24.
64. Cygan JA, Johnson RL, McMahon AP. Novel regulatory interactions revealed by studies of murine limb pattern in Wnt-7a and En-1 mutants. Development. 1997;124(24):5021–32.
65. Loomis CA, Kimmel RA, Tong CX, Michaud J, Joyner AL. Analysis of the genetic pathway leading to formation of ectopic apical ectodermal ridges in mouse Engrailed-1 mutant limbs. Development. 1998;125(6):1137–48.
66. Riddle RD, Ensini M, Nelson C, Tsuchida T, Jessell TM, Tabin C. Induction of the LIM homeobox gene Lmx1 by WNT7a establishes dorsoventral pattern in the vertebrate limb. Cell. 1995;83(4): 631–40.
67. Vogel A, Rodriguez C, Warnken W, Izpisua Belmonte JC. Dorsal cell fate specified by chick Lmx1 during vertebrate limb development. Nature. 1995;378(6558):716–20.
68. Zuniga A, Haramis AP, McMahon AP, Zeller R. Signal relay by BMP antagonism controls the SHH/FGF4 feedback loop in vertebrate limb buds. Nature. 1999;401(6753):598–602.
69. Michos O, Panman L, Vintersten K, Beier K, Zeller R, Zuniga A. Gremlin-mediated BMP antagonism induces the epithelial-mesenchymal feedback signaling controlling metanephric kidney and limb organogenesis. Development. 2004;131(14):3401–10.
70. Bandyopadhyay A, Tsuji K, Cox K, Harfe BD, Rosen V, Tabin CJ. Genetic analysis of the roles of BMP2, BMP4, and BMP7 in limb patterning and skeletogenesis. PLoS Genet. 2006;2(12):e216.
71. Benazet JD, Bischofberger M, Tiecke E, Goncalves A, Martin JF, Zuniga A, Naef F, Zeller R. A self-regulatory system of interlinked signaling feedback loops controls mouse limb patterning. Science. 2009;323(5917):1050–3.
72. Verheyden JM, Sun X. An Fgf/Gremlin inhibitory feedback loop triggers termination of limb bud outgrowth. Nature. 2008; 454(7204):638–41.
73. Yang Y, Niswander L. Interaction between the signaling molecules WNT7a and SHH during vertebrate limb development: dorsal signals regulate anteroposterior patterning. Cell. 1995;80(6):939–47.
74. Fernandez-Teran M, Ros MA, Mariani FV. Evidence that the limb bud ectoderm is required for survival of the underlying mesoderm. Dev Biol. 2013;381(2):11.
75. Woltering JM, Duboule D. The origin of digits: expression patterns versus regulatory mechanisms. Dev Cell. 2010;18(4):526–32.
76. Yokouchi Y, Sasaki H, Kuroiwa A. Homeobox gene expression correlated with the bifurcation process of limb cartilage development. Nature. 1991;353(6343):443–5.
77. Nelson CE, Morgan BA, Burke AC, Laufer E, DiMambro E, Murtaugh LC, Gonzales E, Tessarollo L, Parada LF, Tabin C. Analysis of Hox gene expression in the chick limb bud. Development. 1996;122(5):1449–66.
78. Kmita M, Fraudeau N, Herault Y, Duboule D. Serial deletions and duplications suggest a mechanism for the collinearity of Hoxd genes in limbs. Nature. 2002;420(6912):145–50.
79. Dreyer SD, Naruse T, Morello R, Zabel B, Winterpacht A, Johnson RL, Lee B, Oberg KC. Lmx1b expression during joint and tendon formation: localization and evaluation of potential downstream targets. Gene Expr Patterns. 2004;4(4):397–405.
80. Zeller R. It takes time to make a pinky: unexpected insights into how SHH patterns vertebrate digits. Sci STKE. 2004;2004(259):e53.
81. Harfe BD, Scherz PJ, Nissim S, Tian H, McMahon AP, Tabin CJ. Evidence for an expansion-based temporal Shh gradient in specifying vertebrate digit identities. Cell. 2004;118(4):517–28.
82. Zhu J, Nakamura E, Nguyen MT, Bao X, Akiyama H, Mackem S. Uncoupling Sonic hedgehog control of pattern and expansion of the developing limb bud. Dev Cell. 2008;14(4):624–32.
83. Yang Y, Drossopoulou G, Chuang PT, Duprez D, Marti E, Bumcrot D, Vargesson N, Clarke J, Niswander L, McMahon A, et al. Relationship between dose, distance and time in Sonic Hedgehog-mediated regulation of anteroposterior polarity in the chick limb. Development. 1997;124(21):4393–404.
84. Towers M, Mahood R, Yin Y, Tickle C. Integration of growth and specification in chick wing digit-patterning. Nature. 2008; 452(7189):882–6.
85. Sheth R, Marcon L, Bastida MF, Junco M, Quintana L, Dahn R, Kmita M, Sharpe J, Ros MA. Hox genes regulate digit patterning by controlling the wavelength of a Turing-type mechanism. Science. 2012;338(6113):1476–80.
86. Turing AM. The chemical basis of morphogenesis. 1953. Bull Math Biol. 1990;52(1–2):153–97.
87. Suzuki T, Hasso SM, Fallon JF. Unique SMAD1/5/8 activity at the phalanx-forming region determines digit identity. Proc Natl Acad Sci U S A. 2008;105(11):4185–90.
88. Montero JA, Lorda-Diez CI, Ganan Y, Macias D, Hurle JM. Activin/TGFbeta and BMP crosstalk determines digit chondrogenesis. Dev Biol. 2008;321(2):343–56.
89. Dahn RD, Fallon JF. Interdigital regulation of digit identity and homeotic transformation by modulated BMP signaling. Science. 2000;289(5478):438–41.

90. Chen Y, Knezevic V, Ervin V, Hutson R, Ward Y, Mackem S. Direct interaction with Hoxd proteins reverses Gli3-repressor function to promote digit formation downstream of Shh. Development. 2004;131(10):2339–47.
91. Wang B, Fallon JF, Beachy PA. Hedgehog-regulated processing of Gli3 produces an anterior/posterior repressor gradient in the developing vertebrate limb. Cell. 2000;100(4):423–34.
92. Drossopoulou G, Lewis KE, Sanz-Ezquerro JJ, Nikbakht N, McMahon AP, Hofmann C, Tickle C. A model for anteroposterior patterning of the vertebrate limb based on sequential long- and short-range Shh signalling and Bmp signalling. Development. 2000;127(7):1337–48.
93. Rowe DA, Cairns JM, Fallon JF. Spatial and temporal patterns of cell death in limb bud mesoderm after apical ectodermal ridge removal. Dev Biol. 1982;93(1):83–91.
94. Sanz-Ezquerro JJ, Tickle C. Fgf signaling controls the number of phalanges and tip formation in developing digits. Curr Biol. 2003;13(20):1830–6.
95. Winkel A, Stricker S, Tylzanowski P, Seiffart V, Mundlos S, Gross G, Hoffmann A. Wnt-ligand-dependent interaction of TAK1 (TGF-beta-activated kinase-1) with the receptor tyrosine kinase Ror2 modulates canonical Wnt-signalling. Cell Signal. 2008; 20(11):2134–44.
96. Witte F, Chan D, Economides AN, Mundlos S, Stricker S. Receptor tyrosine kinase-like orphan receptor 2 (ROR2) and Indian hedgehog regulate digit outgrowth mediated by the phalanx-forming region. Proc Natl Acad Sci U S A. 2010;107(32):14211–6.
97. Oberg KC. Review of the molecular development of the thumb: digit primera. Clin Orthop Relat Res. 2014;472(4):1101–5.
98. Koshiba-Takeuchi K, Takeuchi JK, Arruda EP, Kathiriya IS, Mo R, Hui CC, Srivastava D, Bruneau BG. Cooperative and antagonistic interactions between Sall4 and Tbx5 pattern the mouse limb and heart. Nat Genet. 2006;38(2):175–83.
99. Saint-Hilaire IG: Histoire g´en´erale et particuli `ere des anomalies de l'organisation chez l'homme et les animaux. Paris: J.B. Baillière; 1932.
100. Vargas AO, Fallon JF. Birds have dinosaur wings: the molecular evidence. J Exp Zool B Mol Dev Evol. 2005;304(1):86–90.
101. Vargas AO, Kohlsdorf T, Fallon JF, Vandenbrooks J, Wagner GP. The evolution of HoxD-11 expression in the bird wing: insights from Alligator mississippiensis. PLoS One. 2008;3(10): e3325.
102. Villavicencio-Lorini P, Kuss P, Friedrich J, Haupt J, Farooq M, Turkmen S, Duboule D, Hecht J, Mundlos S. Homeobox genes d11-d13 and a13 control mouse autopod cortical bone and joint formation. J Clin Invest. 2010;120(6):1994–2004.
103. Hasson P, DeLaurier A, Bennett M, Grigorieva E, Naiche LA, Papaioannou VE, Mohun TJ, Logan MP. Tbx4 and tbx5 acting in connective tissue are required for limb muscle and tendon patterning. Dev Cell. 2010;18(1):148–56.
104. Casanova JC, Badia-Careaga C, Uribe V, Sanz-Ezquerro JJ. Bambi and Sp8 expression mark digit tips and their absence shows that chick wing digits 2 and 3 are truncated. PLoS One. 2012;7(12): e52781.
105. Casanova JC, Sanz-Ezquerro JJ. Digit morphogenesis: is the tip different? Dev Growth Differ. 2007;49(6):479–91.
106. Kawakami Y, Esteban CR, Matsui T, Rodriguez-Leon J, Kato S, Izpisua Belmonte JC. Sp8 and Sp9, two closely related buttonhead-like transcription factors, regulate Fgf8 expression and limb outgrowth in vertebrate embryos. Development. 2004;131(19):4763–74.
107. Haro E, Delgado I, Hunco M, Yamada Y, Mansouri A, Oberg KC, Ros MA: Sp6 and Sp8 transcription factors control AER formation and Dorsoventral Patterning in Limb Development. PLoS genetics. 2014;In Press.
108. Allan CH, Fleckman P, Fernandes RJ, Hager B, James J, Wisecarver Z, Satterstrom FK, Gutierrez A, Norman A, Pirrone A, et al. Tissue response and Msx1 expression after human fetal digit tip amputation in vitro. Wound Repair Regen. 2006;14(4): 398–404.
109. Han M, Yang X, Farrington JE, Muneoka K. Digit regeneration is regulated by Msx1 and BMP4 in fetal mice. Development. 2003;130(21):5123–32.
110. Yoon BS, Pogue R, Ovchinnikov DA, Yoshii I, Mishina Y, Behringer RR, Lyons KM. BMPs regulate multiple aspects of growth-plate chondrogenesis through opposing actions on FGF pathways. Development. 2006;133(23):4667–78.
111. Cunningham TJ, Chatzi C, Sandell LL, Trainor PA, Duester G. Rdh10 mutants deficient in limb field retinoic acid signaling exhibit normal limb patterning but display interdigital webbing. Dev Dyn. 2011;240(5):1142–50.
112. Rodriguez-Leon J, Merino R, Macias D, Ganan Y, Santesteban E, Hurle JM. Retinoic acid regulates programmed cell death through BMP signalling. Nat Cell Biol. 1999;1(2):125–6.
113. Weatherbee SD, Behringer RR, Rasweiler JJ, Niswander LA. Interdigital webbing retention in bat wings illustrates genetic changes underlying amniote limb diversification. Proc Natl Acad Sci U S A. 2006;103(41):15103–7.
114. Choi K. Hemangioblast development and regulation. Biochem Cell Biol. 1998;76(6):947–56.
115. Nimmagadda S, Geetha Loganathan P, Huang R, Scaal M, Schmidt C, Christ B. BMP4 and noggin control embryonic blood vessel formation by antagonistic regulation of VEGFR-2 (Quek1) expression. Dev Biol. 2005;280(1):100–10.
116. Park C, Afrikanova I, Chung YS, Zhang WJ, Arentson E, Fong Gh G, Rosendahl A, Choi K. A hierarchical order of factors in the generation of FLK1- and SCL-expressing hematopoietic and endothelial progenitors from embryonic stem cells. Development. 2004;131(11):2749–62.
117. Shalaby F, Rossant J, Yamaguchi TP, Gertsenstein M, Wu XF, Breitman ML, Schuh AC. Failure of blood-island formation and vasculogenesis in Flk-1-deficient mice. Nature. 1995;376(6535): 62–6.
118. Shalaby F, Ho J, Stanford WL, Fischer KD, Schuh AC, Schwartz L, Bernstein A, Rossant J. A requirement for Flk1 in primitive and definitive hematopoiesis and vasculogenesis. Cell. 1997;89(6): 981–90.
119. Ferguson M, Byrnes C, Sun L, Marti G, Bonde P, Duncan M, Harmon JW. Wound healing enhancement: electroporation to address a classic problem of military medicine. World J Surg. 2005;29 Suppl 1:S55–9.
120. Drake CJ. Embryonic and adult vasculogenesis. Birth Defects Res C Embryo Today. 2003;69(1):73–82.
121. Moser M, Patterson C. Bone morphogenetic proteins and vascular differentiation: BMPing up vasculogenesis. Thromb Haemost. 2005;94(4):713–8.
122. He L, Papoutsi M, Huang R, Tomarev SI, Christ B, Kurz H, Wilting J. Three different fates of cells migrating from somites into the limb bud. Anat Embryol (Berl). 2003;207(1):29–34.
123. Caplan AI. The vasculature and limb development. Cell Differ. 1985;16(1):1–11.
124. Vargesson N. Vascularization of the developing chick limb bud: role of the TGFbeta signalling pathway. J Anat. 2003;202(1):93–103.
125. Deckers MM, van Bezooijen RL, van der Horst G, Hoogendam J, van Der Bent C, Papapoulos SE, Lowik CW. Bone morphogenetic proteins stimulate angiogenesis through osteoblast-derived vascular endothelial growth factor A. Endocrinology. 2002;143(4): 1545–53.
126. Hellstrom M, Phng LK, Hofmann JJ, Wallgard E, Coultas L, Lindblom P, Alva J, Nilsson AK, Karlsson L, Gaiano N, et al. Dll4 signalling through Notch1 regulates formation of tip cells during angiogenesis. Nature. 2007;445(7129):776–80.
127. Siekmann AF, Lawson ND. Notch signalling limits angiogenic cell behaviour in developing zebrafish arteries. Nature. 2007;445(7129):781–4.
128. Jones CA, Li DY. Common cues regulate neural and vascular patterning. Curr Opin Genet Dev. 2007;17(4):332–6.

129. Thurston G. Role of Angiopoietins and Tie receptor tyrosine kinases in angiogenesis and lymphangiogenesis. Cell Tissue Res. 2003;314(1):61–8.
130. Krebs LT, Xue Y, Norton CR, Shutter JR, Maguire M, Sundberg JP, Gallahan D, Closson V, Kitajewski J, Callahan R, et al. Notch signaling is essential for vascular morphogenesis in mice. Genes Dev. 2000;14(11):1343–52.
131. Tamura K, Amano T, Satoh T, Saito D, Yonei-Tamura S, Yajima H. Expression of rigf, a member of avian VEGF family, correlates with vascular patterning in the developing chick limb bud. Mech Dev. 2003;120(2):199–209.
132. Betsholtz C, Lindblom P, Gerhardt H. Role of pericytes in vascular morphogenesis. EXS. 2005;94:115–25.
133. Ribes V, Otto DM, Dickmann L, Schmidt K, Schuhbaur B, Henderson C, Blomhoff R, Wolf CR, Tickle C, Dolle P. Rescue of cytochrome P450 oxidoreductase (Por) mouse mutants reveals functions in vasculogenesis, brain and limb patterning linked to retinoic acid homeostasis. Dev Biol. 2007;303(1):66–81.
134. Ribes V, Fraulob V, Petkovich M, Dolle P. The oxidizing enzyme CYP26a1 tightly regulates the availability of retinoic acid in the gastrulating mouse embryo to ensure proper head development and vasculogenesis. Dev Dyn. 2007;236(3):644–53.
135. Rodriguez-Niedenfuhr M, Burton GJ, Deu J, Sanudo JR. Development of the arterial pattern in the upper limb of staged human embryos: normal development and anatomic variations. J Anat. 2001;199(Pt 4):407–17.
136. Mrazkova O. Ontogenesis of arterial trunks in the human forearm. Folia Morphol (Praha). 1973;21(2):193–6.
137. Kawakami Y, Rodriguez-Leon J, Belmonte JC. The role of TGFbetas and Sox9 during limb chondrogenesis. Curr Opin Cell Biol. 2006;18(6):723–9.
138. Akiyama H, Chaboissier MC, Martin JF, Schedl A, de Crombrugghe B. The transcription factor Sox9 has essential roles in successive steps of the chondrocyte differentiation pathway and is required for expression of Sox5 and Sox6. Genes Dev. 2002;16(21):2813–28.
139. Lefebvre V, Li P, de Crombrugghe B. A new long form of Sox5 (L-Sox5), Sox6 and Sox9 are coexpressed in chondrogenesis and cooperatively activate the type II collagen gene. EMBO J. 1998;17(19):5718–33.
140. Karsenty G. Transcriptional control of skeletogenesis. Annu Rev Genomics Hum Genet. 2008;9:183–96.
141. Zou H, Wieser R, Massague J, Niswander L. Distinct roles of type I bone morphogenetic protein receptors in the formation and differentiation of cartilage. Genes Dev. 1997;11(17):2191–203.
142. Pizette S, Niswander L. BMPs are required at two steps of limb chondrogenesis: formation of prechondrogenic condensations and their differentiation into chondrocytes. Dev Biol. 2000;219(2): 237–49.
143. Yoon BS, Ovchinnikov DA, Yoshii I, Mishina Y, Behringer RR, Lyons KM. Bmpr1a and Bmpr1b have overlapping functions and are essential for chondrogenesis in vivo. Proc Natl Acad Sci U S A. 2005;102(14):5062–7.
144. Bandyopadhyay A, Yadav PS, Prashar P. BMP signaling in development and diseases: a pharmacological perspective. Biochem Pharmacol. 2013;85(7):857–64.
145. Weston AD, Rosen V, Chandraratna RA, Underhill TM. Regulation of skeletal progenitor differentiation by the BMP and retinoid signaling pathways. J Cell Biol. 2000;148(4):679–90.
146. Weston AD, Chandraratna RA, Torchia J, Underhill TM. Requirement for RAR-mediated gene repression in skeletal progenitor differentiation. J Cell Biol. 2002;158(1):39–51.
147. Dranse HJ, Sampaio AV, Petkovich M, Underhill TM. Genetic deletion of Cyp26b1 negatively impacts limb skeletogenesis by inhibiting chondrogenesis. J Cell Sci. 2011;124(Pt 16):2723–34.
148. Hoffman LM, Garcha K, Karamboulas K, Cowan MF, Drysdale LM, Horton WA, Underhill TM. BMP action in skeletogenesis involves attenuation of retinoid signaling. J Cell Biol. 2006;174(1): 101–13.
149. Gray DJ, Gardner E, O'Rahilly R. The prenatal development of the skeleton and joints of the human hand. Am J Anat. 1957;101(2):169–223.
150. Shubin NH, Alberch P. A morphogenetic approach to the origin and basic organization of the tetrapod limb. In: Evolutionary Biology. New York: Plenum Press; 1986. p. 319–87.
151. Hinchliffe JR, Johnson DR. The development of the vertebrate limb. Oxford: Clarendon; 1980.
152. Kim IS, Otto F, Zabel B, Mundlos S. Regulation of chondrocyte differentiation by Cbfa1. Mech Dev. 1999;80(2):159–70.
153. Nakashima K, Zhou X, Kunkel G, Zhang Z, Deng JM, Behringer RR, de Crombrugghe B. The novel zinc finger-containing transcription factor osterix is required for osteoblast differentiation and bone formation. Cell. 2002;108(1):17–29.
154. Yang X, Matsuda K, Bialek P, Jacquot S, Masuoka HC, Schinke T, Li L, Brancorsini S, Sassone-Corsi P, Townes TM, et al. ATF4 is a substrate of RSK2 and an essential regulator of osteoblast biology; implication for Coffin-Lowry Syndrome. Cell. 2004; 117(3): 387–98.
155. Mackie EJ, Ahmed YA, Tatarczuch L, Chen KS, Mirams M. Endochondral ossification: how cartilage is converted into bone in the developing skeleton. Int J Biochem Cell Biol. 2008; 40(1):46–62.
156. Noback CR, Robertson GG. Sequences of appearance of ossification centers in the human skeleton during the first five prenatal months. Am J Anat. 1951;89(1):1–28.
157. Stuart HC, Pyle SI, Cornoni J, Reed RB. Onsets, completions and spans of ossification in the 29 bone growth centers of the hand and wrist. Pediatrics. 1962;29:237–49.
158. Hartmann C, Tabin CJ. Wnt-14 plays a pivotal role in inducing synovial joint formation in the developing appendicular skeleton. Cell. 2001;104(3):341–51.
159. Storm EE, Kingsley DM. GDF5 coordinates bone and joint formation during digit development. Dev Biol. 1999;209(1):11–27.
160. Dalgleish AE. Development of the limbs of the mouse. Stanford: Stanford University; 1964.
161. Craig FM, Bayliss MT, Bentley G, Archer CW. A role for hyaluronan in joint development. J Anat. 1990;171(4):17–23.
162. Nowlan NC, Sharpe J, Roddy KA, Prendergast PJ, Murphy P. Mechanobiology of embryonic skeletal development: Insights from animal models. Birth Defects Res C Embryo Today. 2010;90(3):203–13.
163. Khan IM, Redman SN, Williams R, Dowthwaite GP, Oldfield SF, Archer CW. The development of synovial joints. Curr Top Dev Biol. 2007;79:1–36.
164. Pacifici M, Koyama E, Iwamoto M. Mechanisms of synovial joint and articular cartilage formation: recent advances, but many lingering mysteries. Birth Defects Res C Embryo Today. 2005;75(3):237–48.
165. Tozer S, Duprez D. Tendon and ligament: development, repair and disease. Birth Defects Res C Embryo Today. 2005;75(3):226–36.
166. Mitrovic D. Development of the diarthrodial joints in the rat embryo. Am J Anat. 1978;151(4):475–85.
167. Sharma K, Izpisua Belmonte JC. Development of the limb neuromuscular system. Curr Opin Cell Biol. 2001;13(2):204–10.
168. Schweitzer R, Chyung JH, Murtaugh LC, Brent AE, Rosen V, Olson EN, Lassar A, Tabin CJ. Analysis of the tendon cell fate using Scleraxis, a specific marker for tendons and ligaments. Development. 2001;128(19):3855–66.
169. Ros MA, Rivero FB, Hinchliffe JR, Hurle JM. Immunohistological and ultrastructural study of the developing tendons of the avian foot. Anat Embryol (Berl). 1995;192(6):483–96.
170. Kardon G. Muscle and tendon morphogenesis in the avian hind limb. Development. 1998;125(20):4019–32.

171. Edom-Vovard F, Duprez D. Signals regulating tendon formation during chick embryonic development. Dev Dyn. 2004;229(3): 449–57.
172. Murphy M, Kardon G. Origin of vertebrate limb muscle: the role of progenitor and myoblast populations. Curr Top Dev Biol. 2011;96:1–32.
173. Williams BA, Ordahl CP. Pax-3 expression in segmental mesoderm marks early stages in myogenic cell specification. Development. 1994;120(4):785–96.
174. Buckingham M, Bajard L, Chang T, Daubas P, Hadchouel J, Meilhac S, Montarras D, Rocancourt D, Relaix F. The formation of skeletal muscle: from somite to limb. J Anat. 2003;202(1): 59–68.
175. Sze LY, Lee KK, Webb SE, Li Z, Paulin D. Migration of myogenic cells from the somites to the fore-limb buds of developing mouse embryos. Dev Dyn. 1995;203(3):324–36.
176. Bober E, Franz T, Arnold HH, Gruss P, Tremblay P. Pax-3 is required for the development of limb muscles: a possible role for the migration of dermomyotomal muscle progenitor cells. Development. 1994;120(3):603–12.
177. Dietrich S, Abou-Rebyeh F, Brohmann H, Bladt F, Sonnenberg-Riethmacher E, Yamaai T, Lumsden A, Brand-Saberi B, Birchmeier C. The role of SF/HGF and c-Met in the development of skeletal muscle. Development. 1999;126(8):1621–9.
178. Bladt F, Riethmacher D, Isenmann S, Aguzzi A, Birchmeier C. Essential role for the c-met receptor in the migration of myogenic precursor cells into the limb bud. Nature. 1995;376(6543):768–71.
179. Brand-Saberi B, Muller TS, Wilting J, Christ B, Birchmeier C. Scatter factor/hepatocyte growth factor (SF/HGF) induces emigration of myogenic cells at interlimb level in vivo. Dev Biol. 1996;179(1):303–8.
180. Scaal M, Bonafede A, Dathe V, Sachs M, Cann G, Christ B, Brand-Saberi B. SF/HGF is a mediator between limb patterning and muscle development. Development. 1999;126(21):4885–93.
181. Epstein JA, Shapiro DN, Cheng J, Lam PY, Maas RL. Pax3 modulates expression of the c-Met receptor during limb muscle development. Proc Natl Acad Sci U S A. 1996;93(9):4213–8.
182. Schmidt C, Bladt F, Goedecke S, Brinkmann V, Zschiesche W, Sharpe M, Gherardi E, Birchmeier C. Scatter factor/hepatocyte growth factor is essential for liver development. Nature. 1995;373(6516):699–702.
183. Schafer K, Braun T. Early specification of limb muscle precursor cells by the homeobox gene Lbx1h. Nat Genet. 1999;23(2):213–6.
184. Tajbakhsh S, Buckingham ME. Mouse limb muscle is determined in the absence of the earliest myogenic factor myf-5. Proc Natl Acad Sci U S A. 1994;91(2):747–51.
185. Ontell M, Kozeka K. The organogenesis of murine striated muscle: a cytoarchitectural study. Am J Anat. 1984;171(2):133–48.
186. Otto A, Collins-Hooper H, Patel K. The origin, molecular regulation and therapeutic potential of myogenic stem cell populations. J Anat. 2009;215(5):477–97.
187. Dieu T, Newgreen D. Chicken wings and the brachial plexus. Neurol Res. 2007;29(3):225–30.
188. Wehrle-Haller B, Koch M, Baumgartner S, Spring J, Chiquet M. Nerve-dependent and -independent tenascin expression in the developing chick limb bud. Development. 1991;112(2):627–37.
189. Swanson GJ, Lewis J. Sensory nerve routes in chick wing buds deprived of motor innervation. J Embryol Exp Morphol. 1986;95:37–52.
190. Swanson GJ. Paths taken sensory nerve fibres in aneural chick wing buds. J Embryol Exp Morphol. 1985;86:109–24.
191. Martin P, Khan A, Lewis J. Cutaneous nerves of the embryonic chick wing do not develop in regions denuded of ectoderm. Development. 1989;106(2):335–46.
192. Lewis J, Chevallier A, Kieny M, Wolpert L. Muscle nerve branches do not develop in chick wings devoid of muscle. J Embryol Exp Morphol. 1981;64:211–32.
193. Polleux F, Ince-Dunn G, Ghosh A. Transcriptional regulation of vertebrate axon guidance and synapse formation. Nat Rev Neurosci. 2007;8(5):331–40.
194. Dasen JS, Jessell TM. Hox networks and the origins of motor neuron diversity. Curr Top Dev Biol. 2009;88:169–200.
195. Kao TJ, Law C, Kania A. Eph and ephrin signaling: lessons learned from spinal motor neurons. Semin Cell Dev Biol. 2012;23(1):83–91.
196. Dasen JS. Transcriptional networks in the early development of sensory-motor circuits. Curr Top Dev Biol. 2009;87:119–48.
197. Manske PR, Oberg KC. Classification and developmental biology of congenital anomalies of the hand and upper extremity. J Bone Joint Surg Am. 2009;91 Suppl 4:3–18.
198. Tonkin MA, Oberg KC. Congenital hand I—embryology, classification, and principles. In: Cheng J, Neligan PC, editors. Plastic surgery, vol 6: hand and upper extremity. 3rd ed. New York: Elsevier; 2012. p. 526–47.
199. Saint-Hilaire IG. Propositions sur la monstruosité. Paris: Imp. Didot le Jeune; 1829.
200. Saint-Hilaire IG. Histoire générale et particuli ère des anomalies de l'organisation chez l'homme et les animaux. Paris: J.B. Baillière; 1932.
201. Swanson AB. A classification for congenital malformations of the hand. N J Bull Acad Med. 1964;10:166–9.
202. Lösch GM, Buck-Gramcko D, Cihak R, Sharader M, Seichert V. An attempt to classify the malformations of the hand based on morphogenetic criteria. Chir Plastica. 1984;8(1):18.
203. Temtamy SA. Genetic factors in hand malformations. Baltimore: Johns Hopkins University; 1966.
204. Temtamy SA, McKusick VA. The genetics of hand malformations. Birth Defects Orig Artic Ser. 1978;14(3):i–619.
205. Kay H. A proposed international terminology for the classification of congenital limb deficiencies. ICIB/JACPOC. 1974;13(7):1–16.
206. Kelikian H. Congenital deformities of the hand and forearm. Philadelphia: WB Saunders Company; 1974.
207. Knight SL, Kay SPJ. Classification of congenital anomalies. In: Gupta A, Kay SPJ, Scheker LR, editors. The growing hand. London: Harcourt; 2000. p. 125–35.
208. Tonkin MA. Description of congenital hand anomalies: a personal view. J Hand Surg Br. 2006;31(5):489–97.
209. Oberg KC, Feenstra JM, Manske PR, Tonkin MA. Developmental biology and classification of congenital anomalies of the hand and upper extremity. J Hand Surg Am. 2010;35(12):2066–76.
210. Ogino T. JSSH CHCot: modified IFSSH classification. J Jpn Soc Surg Hand. 2000;17:353–65.
211. Tonkin MA, Tolerton SK, Quick TJ, Harvey I, Lawson RD, Smith NC, Oberg KC. Classification of congenital anomalies of the hand and upper limb: development and assessment of a new system. J Hand Surg Am. 2013;13:10.
212. Ezaki M, Baek GH, Horii E, Hovius SE. Classification of congenital hand and upper limb anomalies. In: Ezaki M, editor. Scientific committee on congenital conditions, vol. 14. IFSSH Ezine; 2014. p. 4.
213. Ekblom AG, Laurell T, Arner M. Epidemiology of congenital upper limb anomalies in Stockholm, Sweden, 1997 to 2007: application of the Oberg, Manske, and Tonkin classification. J Hand Surg. 2014;39(2):237–48.
214. Oberg KC, Feenstra JM, Manske PR, Tonkin MA. A new classification of congenital anomalies of the hand and upper limb. IFSSH Ezine. 2011;1(2):3.